

Oxford Research Encyclopedia of Neuroscience

The Functional Organization of Vertebrate Retinal Circuits for Vision

Tom Baden, Timm Schubert, Philipp Berens, and Thomas Euler

Subject: Computational Neuroscience, Sensory Systems Online Publication Date: Mar 2018

DOI: 10.1093/acrefore/9780190264086.013.68

Summary and Keywords

Visual processing begins in the retina—a thin, multilayered neuronal tissue lining the back of the vertebrate eye. The retina does not merely read out the constant stream of photons impinging on its dense array of photoreceptor cells. Instead it performs a first, extensive analysis of the visual scene, while constantly adapting its sensitivity range to the input statistics, such as the brightness or contrast distribution. The functional organization of the retina abides to several key organizational principles. These include overlapping and repeating instances of both divergence and convergence, constant and dynamic range-adjustments, and (perhaps most importantly) decomposition of image information into parallel channels. This is often referred to as “parallel processing.” To support this, the retina features a large diversity of neurons organized in functionally overlapping microcircuits that typically uniformly sample the retinal surface in a regular mosaic. Ultimately, each circuit drives spike trains in the retina’s output neurons, the retinal ganglion cells. Their axons form the optic nerve to convey multiple, distinctive, and often already heavily processed views of the world to higher visual centers in the brain.

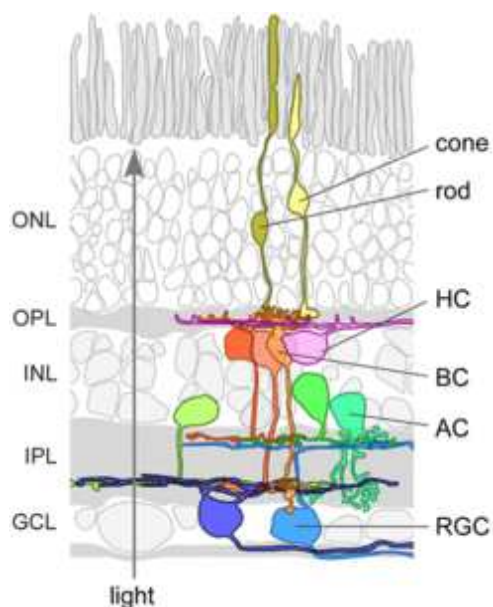
From an experimental point of view, the retina is a neuroscientist’s dream. While part of the central nervous system, the retina is largely self-contained, and depending on the species, it receives little feedback from downstream stages. This means that the tissue can be disconnected from the rest of the brain and studied in a dish for many hours without losing its functional integrity, all while retaining excellent experimental control over the exclusive natural network input: the visual stimulus. Once removed from the eyecup, the retina can be flattened, thus its neurons are easily accessed optically or using visually guided electrodes. Retinal tiling means that function studied at any one place can usually be considered representative for the entire tissue. At the same time, species-dependent specializations offer the opportunity to study circuits adapted to different visual tasks: for example, in case of our fovea, high-acuity vision. Taken together, today the retina is amongst the best understood complex neuronal tissues of the vertebrate brain.

Keywords: vision, retina, parallel processing, divergence, convergence, feed-forward network, dynamic range, synapse

Overview

The retina is made up of five classes of neurons—photoreceptors, horizontal cells, amacrine cells, bipolar cells,

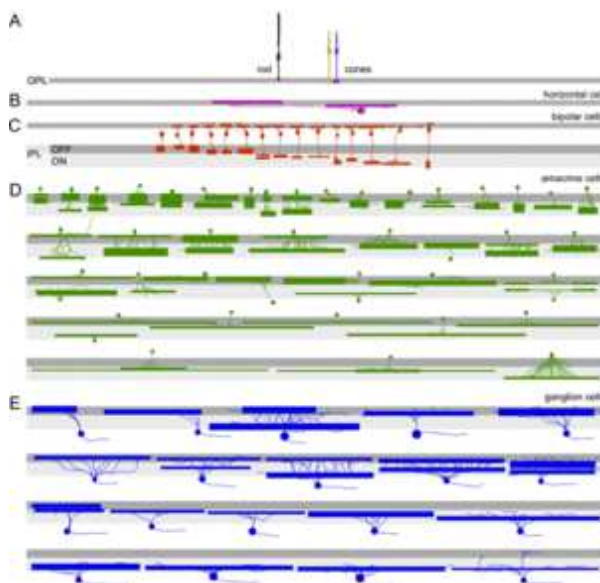
ganglion cells—that interact in two synaptic layers: the outer and the inner plexiform layers (OPL, IPL) (Masland, 2001; Wässle, 2004) (see Figure 1). It is here where most of the network’s computational power resides. In the outer retina, photoreceptors express light-sensitive proteins called opsins, which are extremely densely packed in their outer segments (Fu & Yau, 2007). A complex, highly regulated transduction cascade that starts with the opsin translates the stream of incoming photons into graded changes in membrane potential (Goldberg et al., 2016; Koch, 1992; Fain et al., 2001; Yau et al., 2009). Photoreceptors employ ribbon synapses to constantly release the neurotransmitter glutamate in the dark and reduce glutamate release as light level increases (Sterling & Matthews, 2005). Their synaptic output drives two classes of neurons in the OPL: horizontal cells (HCs) and bipolar cells (BCs). HCs are large, laterally connecting inhibitory neurons that provide both feedback and feed-forward inputs to photoreceptor terminals as well as feed-forward inputs to BC dendrites (Peichl et al., 1998). Bipolar cells, on the other hand, connect the OPL with the IPL (Euler et al., 2014). They integrate inputs from photoreceptors and HCs at their dendrites and project to the inner retina, where they use also ribbon synapses to release glutamate onto the remaining two classes of neurons: Amacrine cells (ACs) (Vaney, 1990; Masland, 1988) and retinal ganglion cells (RGCs) (Dhande & Huberman, 2014). With a few exceptions, ACs are inhibitory; they interconnect neurons both laterally and vertically within the IPL. Finally, RGCs integrate information typically across many BCs and ACs and subsequently send information to the brain via their long axons that form the optic nerve.



Click to view larger

Figure 1. Schematic drawing of a mouse retina in side view. Two plexiform layers with synaptic connections (OPL, outer plexiform layer; IPL, inner plexiform layer) separate three cellular layers, the inner and the outer nuclear layer (INL, ONL) and the ganglion cell layer (GCL). The arrow indicates the direction of the light falling into the eye. Cone and rod photoreceptors (yellow) send light signals to the dendrites of the bipolar cells (BC, orange), which form synapses with the dendrites of the retinal ganglion cells (RGC, blue). Their axons form the optic nerve. Horizontal cells (HC, lilac) and amacrine cells (AC, green) modulate the signals of bipolar and ganglion cells in the OPL and the IPL, respectively.

Each of the five classes of retinal neurons is usually made up of multiple types (Figure 2). For example, a typical non-primate mammalian retina harbors three types of photoreceptors: two types of cone photoreceptors (cones) and one type of rod photoreceptor (rods) (Pugh & Lamb, 2000). While there are a number of anatomical and functional differences between these neurons, the perhaps most critical are which type of opsin protein is expressed and how the transduction cascade that couples this opsin to changes in photoreceptor membrane potential is tuned (Goldberg et al., 2016; Arshavsky et al., 2002). Fundamentally, the rod version of this process has a higher gain than the cone version. As a result, rods operate best at low-light levels (night or “scotopic” vision) but saturate as the light becomes too bright (daylight or “photopic” vision), the regime where cones take over. At transition levels, both rods and cones can be active (“mesopic” vision). Signals from rods are integrated later in the network through the so-called primary rod-pathway which involves a specialized rod-BC as well as a dedicated AC (Euler et al., 2014; Dacheux & Raviola, 1986). In addition, rod signals can also feed into the retinal network via gap-junctions with cones and by direct contacts with some types of cone-bipolar cell. Among the cone types, differences between the opsins expressed result in different spectral sensitivities, thereby forming the basis of color vision.



[Click to view larger](#)

Figure 2. Mouse retina inventory. Illustration showing the (incomplete) complement of mouse retinal neurons in side view. For each cell type, stratification depth and width, as well as lateral extent of axon terminal system (cones, rod, horizontal cell, bipolar cells) or dendritic arbor (horizontal cell, amacrine cells, ganglion cells) is approximated by bars. A,B, one type of rod photoreceptor and two types of cone photoreceptors (A); one type of horizontal cell. C, the anatomical survey of mouse bipolar cell (BC) types is considered completed (BCs adapted from (Behrens et al., 2016); with glutamatergic monopolar interneuron (GluMI, leftmost cell) added based on (Shekhar et al., 2016; Santina et al., 2016). D, so far, for mouse amacrine cells (ACs), no exhaustive survey exists that includes both small- and large-field groups; the panel shows the set of AC types adapted from cells reconstructed in an electron microscopy (EM) data set (Helmstaedter et al., 2013). Because the EM data set comprised only a relatively small tissue block, the dendritic arbor diameters of depicted wide-field ACs are likely underestimates. E, while several morphological surveys exist for mouse retinal ganglion cells (RGCs) (i.e., Sun et al., 2002; Völgyi et al., 2009; Sümbül et al., 2014; Kong et al., 2005; Coombs et al., 2006), a systematic consolidation of the described types as well as a unified nomenclature is still missing. Hence, an exemplary selection of RGCs is shown, likely representing approximately half of the morphological RGC types (for discussion, see Sanes & Masland, 2014; cells adapted from Baden et al., 2016).

will focus on the following key aspects:

1) Adaptation. The retina continuously responds to changes in its input statistics to keep the network within its dynamic range.

2) Noise reduction. Sources of noise need to be suppressed (or averaged out) to ensure faithful transmission

The remaining four classes of retinal neurons also consist of multiple types—often several dozens of them. For example, mice possess 14 types of BCs (Wässle et al., 2009; Helmstaedter et al., 2013; Greene et al., 2016; Ghosh et al., 2004) and two to three times that number of RGCs (Baden et al., 2016) (see Figure 2). In general, cell-type diversity increases as the signals trickle through the retinal network. Depending on the species, a handful of photoreceptor and HC types feed into one or two dozen BCs, which in turn connect with often more than 30 to 45 types of RGC (Robles et al., 2014; Baden et al., 2016) and AC (Helmstaedter et al., 2013) each. This “numerical divergence,” along with its functional consequence (parallelization) are fundamental organizational principles of retinal design (Wässle, 2004): The visual stimulus is first picked up by a few broadly tuned photoreceptor cells to ultimately end up represented in parallel by many, much more specifically tuned neurons. However, from the point of view of most retinal neurons, there is a net convergence of inputs: single bipolar cells typically integrate over 10s of photoreceptors, while retinal ganglion cells can combine inputs from hundreds of bipolar cells. In a simplified view, the retina might be compared to a “series of filters” implemented by its individual cell types or their cellular compartments, starting with “general filtering” in the outer retina and then increasingly “specific filtering” in the inner retina (Meister & Berry, 1999). The result is a retinal output that consists of multiple parallel streams (“information channels”), each informing the brain about the presence and location of a particular set of “features” in the visual world. These features may vary dramatically in complexity, starting perhaps from a simple change in contrast in space or time, to the specific encoding of object or field motion in one direction and at a particular speed. Accordingly, much of the retina’s organization is geared to differentially process the visual signal through its many output channels, long before this information is being sent to the visual areas of the brain. In this review, we

of the visual scene to the brain.

3) Feature computation. The retina extracts important and/or surprising visual features in the input and selectively conveys these to the brain, while discarding redundant or expected information.

4) Color vision. In addition to providing a pure intensity-based (greyscale) representation of the outside world, most visual systems can also tell wavelength independent of intensity, thus laying the foundations for color vision.

5) Environmental adaptations. A species' retina usually features specializations to better operate within the animal's unique visual environment.

Adaptation

Like most sensory systems, the eye needs to cope with a vast range of physical attributes in the stimulus (Laughlin, 1989; Demb, 2008). For example, between a nearly pitch-black hole in the ground and direct sunlight a terrestrial diurnal animal may need to cope with a difference in overall light intensity of an order of 10^{8-9} (Hoefflinger, 2007; Luo et al., 2008). However, limits on absolute spike rates or, in the case of graded encoding, limits on the achievable signal-to-noise ratio, dictate that most individual neurons can only meaningfully encode stimulus changes over one to two orders of magnitude (Naka & Rushton, 1966; Normann & Perlman, 1979). If the stimulus exceeds that range in either direction, the neuron needs to settle into a new operational range. Alternatively, differentially tuned neurons or circuits must take over. The retina pursues both strategies.

First, as noted above, rods and cones are tuned to operate under different yet overlapping regimes of brightness (Fain et al., 2001; Kefalov et al., 2003; Leskov et al., 2000). Accordingly, simply by using different types of photoreceptor in parallel most visual vertebrates have found a way to substantially increase the full range of intensities their eyes can cope with. However, each of the photoreceptor systems alone can encode intensities well beyond the limit of two orders of magnitude of a single non-adapting neuron. This capability requires a form of “memory” of recent stimulus history (i.e., tracking the mean light intensity). In the retina, this is implemented by a range of mechanisms that operate at different time-scales and utilise different intracellular and synaptic components. For example, photoreceptors themselves feature a built-in “automatic gain control,” simply as each photoisomerisation event is followed by a recovery period of several minutes (Redmond et al., 1998; Fain et al., 2001). Therefore, the more photons hit a photoreceptor, the higher the fraction of non-responsive (“bleached”) opsins. Thus, the photoreceptor's overall sensitivity falls and reaches an equilibrium with current light intensity within a few seconds. Once light intensity drops again, the fraction of recovered opsins increases and so does the photoreceptor overall sensitivity. Pigment bleaching adaptation is but one of many mechanisms of adaptation used by photoreceptors. In fact, different forms of adaptation shift in impact depending on overall brightness and recent stimulus history (Fain et al., 2001). For example, while pigment bleaching is the predominant adaptation mechanism for bright light conditions, a series of feedback loops that aim at optimal light adaptation at low-to-moderate light levels are implemented in the transduction cascade (Normann & Perlman, 1979; Soo et al., 2008) including modulation of calcium and cGMP levels (Burkhardt, 1994). In addition, the output gain at the photoreceptor synapse is modulated by intrinsic (Xu & Slaughter, 2005; Barnes et al., 1993; DeVries, 2001) and/or synaptic (reviewed in Thoreson & Mangel, 2012; Chapot et al., 2017) adaptational mechanisms.

The role of HCs in adaptation is less clear. Nonetheless, they control PR output by a range of mechanisms. BCs dendrites and HC processes form a synaptic complex with the photoreceptor axon terminal (Haverkamp et al.,

2000). Three unusual, interlinked synaptic feedback mechanisms from HCs to the photoreceptor—ephaptic, pH-mediated and GABA (auto-)reception—regulate the gain of glutamate release by from the photoreceptor synapse (Vroman et al., 2014; Liu et al., 2013; Jackman et al., 2011; Kemmler et al., 2014). The different mechanisms may be related to a need for feedback over a wide range of timescales and possibly to species differences. In addition, photoreceptor release is not only modulated by local but also by global feedback from HCs as well as by neighboring cones via glutamate spill-over (Szmajda & DeVries, 2011; Vroman & Kamermans, 2015). The complex synaptic interactions at the photoreceptor axon terminal likely reflect the importance of strictly regulating this synapse for keeping the visual system “running.”

Conceptually similar forms of adaptation to light intensity occur at several stages of the retinal network, but the cellular and molecular mechanisms employed (and thus also their time scales and sensitivity regimes) differ widely (Demb, 2008). As a rule of thumb, later network elements tend to feature faster and more sensitive adaptation mechanisms—an organizational principle that ensures that downstream neurons that can pool over more presynaptic elements and thus keep noise levels low are quicker to adapt to subtle changes in intensity (Dunn et al., 2007).

Beyond adaptation to light intensity, retinal circuits adapt to a range of other features in the visual input (Webster, 2011; Demb, 2002). One notable example is contrast adaptation (i.e., the adaptation to the variance of a stimulus rather than its mean) (Shapley & Victor, 1978). Here, several different mechanisms located in both inner and outer retina come into play (Demb, 2008; Baccus & Meister, 2002; Liu et al., 2015). So-called fast contrast adaptation, often referred to as “contrast gain control,” occurs within the first few hundreds of milliseconds following a change in contrast. The underlying mechanisms involve both BCs and RGCs (Wark et al., 2009; Kastner & Baccus, 2013). Next, “slow contrast adaptation” occurs over a time scale of seconds to tens of seconds and involves the inner retinal neurites of BCs, ACs, as well as RGCs. Within the terminal of BCs, an increase in contrast results in a gradual depletion of vesicles available for fusion, thus reducing the excitatory drive to RGCs (Nikolaev et al., 2013; Manookin & Demb, 2006). In tandem, inhibition received from ACs also adapts (Vickers et al., 2012). Accordingly, depending on the initial strength of inhibition and the relative rates of change of both processes, the result can even be an effective sensitization to contrast (Nikolaev et al., 2013) (see also discussion in Kastner & Baccus, 2013).

Finally, also RGCs can contribute. In their dendrites, increased contrast can trigger the build up of a slowly decaying after-hyperpolarization that effectively counteracts its received excitatory drive (Weick & Demb, 2011, Kim & Rieke, 2003). Moreover, depending on the set of voltage-gated Na^+ channels expressed, the RGC spike generator can contribute to contrast adaptation (Mobbs et al., 1992; Kim & Rieke, 2003).

Network adaptations to a change in input or environmental variables can also come from a different source altogether: neuromodulation. Like any neural tissue, the retina is constantly bathed in a complex cocktail of substances that traverse traditional synaptic boundaries. These include dopamine (Boelen et al., 1998; Esposti et al., 2013; Dowling, 1991; Qiao et al., 2016), substance-P (Kolb et al., 1995), retinoic acid (Weiler et al., 1998), and acetylcholine (Masland, Mills, & Cassidy, 1984; Masland, Mills, & Hayden, 1984), as well as a wealth of endocannabinoids (Yazulla, 2008; Miraucourt et al., 2016). Each of these substances can act on several sites within the network at a time by volume transmission, often with differential downstream effects based on differential receptor expression in subsets of retinal neurons (Farshi et al., 2015). For example, dopamine released by dopaminergic amacrine cells modulates electrical coupling among photoreceptors (Jin et al., 2015), HCs in the outer (Mangel & Dowling, 1985; He et al., 2000) and ACs in the inner retina (Kothmann et al., 2009; Urschel et al., 2006), affecting, for instance, receptive field sizes. Moreover, dopamine likely affects synaptic activity by

modulating voltage-gated Ca^{2+} channels in HCs (Liu et al., 2016) and therefore, in turn, light adaptation.

Taken together, the retina appears to use every opportunity to implement mechanisms that maintain its operating range tuned to recent stimulus history, from tweaking biochemical pathways to adjusting the rules that govern overall network connectivity and which cells partake in specific tasks. However, beyond changes in overall brightness and its variance, natural visual scenes differ by a great number of higher order visual statistics (Geisler, 2008), which for efficient coding should also be reflected in retinal mechanisms of adaptation. If and how these higher order statistics are reflected in retinal adaptation remains one major frontier in the field and likely will continue to do so for a long time. Similarly, how different known (and unknown) mechanisms functionally interact to deliver a stable view of the world remains an active area of research.

Noise Reduction

Like all signal processing “devices,” also neuronal networks suffer from noise (Sterling & Laughlin, 2016). In the retina, this begins with the transduction process itself (Barlow, 1956; Donner, 1992; Yau et al., 2009; Baylor et al., 1979). The light-sensitive component in the opsin (11-cis-retinal) can also isomerise spontaneously (due to thermal activation) rather in response to an absorbed photon (Baylor et al., 1980). Therefore, already the phototransduction cascade that links the opsin activation to a modulation of membrane channels is inherently noisy. This problem becomes particularly relevant at low light levels (“dark noise”). Further downstream, several other sources of noise exist, including further sources of photo-transduction noise (Yau et al., 1979; Matthews & Watanabe, 1987). Another source is synaptic noise (Angueyra & Rieke, 2013; Ala-Laurila et al., 2011), which can be caused by synaptic vesicles spontaneously fusing in the absence of a stimulus, or failing to fuse in its presence. To deal with these and many other sources of noise, the retina pursues three non-mutually exclusive main strategies: averaging-out noise by (1) pooling upstream signals or (2) using long integration times, or (3) cutting of noise by thresholding (Figure 3).

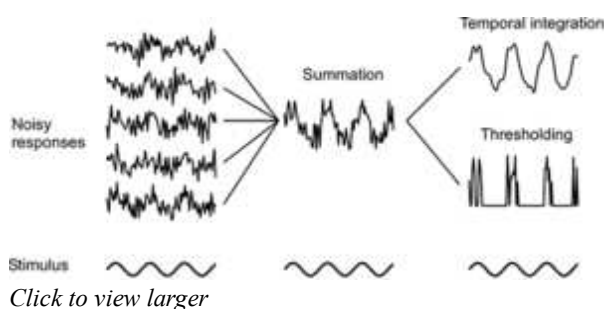


Figure 3. Strategies for reducing noise. Responses of early retinal neurons are typically noisier (left) than those of later neurons, which can pool across multiple inputs to average out some of the noise (center). In addition, slow integration times allow reducing noise at the expense of temporal fidelity (right, top), while thresholding can be used to cut noise (right, bottom).

The first strategy takes several upstream elements and sums up their signals in fewer downstream neurons. The retinal architecture features several instances of such convergence: From photoreceptors to HCs and BCs, from BCs to RGCs and ACs but also from HCs to BCs and from ACs to other ACs and RGCs. For example, most BCs make synaptic connections to several individual photoreceptors (Li et al., 2012; Wässle et al., 2009; Behrens et al., 2016). Therefore, small fluctuations in the output of an individual photoreceptor are drowned out in the chorus of the other inputs and synchronous inputs from many photoreceptors have a much better chance of getting through. This ensures a high signal-to-noise representation of salient features in the input. On the downside, small “meaningful”

perturbations in only one or few upstream elements are more easily lost.

Since synchronization therefore aids signal propagation, mechanisms that laterally connect neurons belonging to

a common circuit become particularly relevant. Most notably, this pertains to electrical coupling via specialized inter-cellular protein channels (“gap junctions”) between retinal neurons. Gap-junctional electrical coupling in the retina occurs at several stages, involving examples from all five classes of neurons (Arai et al., 2010; Völgyi et al., 2009; Mills & Massey, 1995; Vaney et al., 1998; Cook & Becker, 1995).

Input noise can also be ameliorated using a temporal mechanism (i.e., temporal integration). For example, presynaptic release due to a single isomerisation event from rods is smeared out in time compared to that of cones, meaning that postsynaptic rod BCs have more time to integrate inputs than cone BCs (Hensley et al., 1993). As a result, rod BCs are better suited to encode slow events, yet at higher signal-to-noise. A real-world consequence of this is, for example, the difficulty of hitting an incoming tennis ball at low light levels.

Finally, noise reduction through thresholding assumes that a fraction of incoming signal can be discarded entirely at the benefit of also losing its associated noise. A classic example of this process is spike generation, as used by all RGCs as well as several types of BC and AC. By requiring a minimum activation level before a signal is being passed on, spiking neurons categorically cut low-level input noise, although at the expense of losing any information contained alongside. Other cellular processes also can implement this type of noise filtering. For instance, at light levels near visual threshold, the rod-to-rod BC synapse is extremely non-linear, effectively truncating the propagation of individual isomerization events (Field & Rieke, 2002). At the extreme end, neurons can exhibit stochastic resonance (Shimokawa et al., 1999). Here, the threshold is set so high that any depolarisation due to the hypothetical noise-free signal (generator potential) by itself is insufficient to trigger signal propagation. Only if both the generator potential plus the noise are simultaneously high does the neuron fire. The result is a system that exhibits very high temporal precision with an extremely low rate of false-positives: however, this is at the expense of a high rate of false-negatives (Baden et al., 2011, 2014). At least in principle, the latter can be to some extent remedied by pooling, as in the case of many sparsely spiking BCs converging onto individual, much larger RGCs (Baden & Euler, 2013; Baden et al., 2011) (see Figure 4B).

Taken together, the main strategies to limit the propagation of noise through the network all favor larger over smaller inputs. Therefore, preserving also low amplitude signals requires parallelization. Rather than building all retinal output channels based on the same noise suppression strategies, the network instead sets up differentially noisy channels in parallel. For example, the midget system of the primate central fovea uses no convergence at all: A single cone feeds into a single midget BC, which in turn drives its dedicated RGC (Kolb & Marshak, 2003). Beside spike generation in the midget RGC itself, and nonlinear synaptic transfer from the midget bipolar cell, there is little this circuit can do about noise. In comparison, the circuit of the parasol RGCs features several instances of convergence (as well as thresholding) to ultimately yield a fast, high signal-to-noise channel, albeit at substantially reduced spatial resolution (Jacoby et al., 1996).

In the future, it will be important to acknowledge not only noise sources when considering the performance of retinal circuits (e.g., using computational models) but also the networks’ diverse noise suppression strategies. Also on the visual stimulus side, it is crucial to go beyond simple, “synthetic” stimuli and instead use more naturalistic ones, which include more noise. That the retina can recruit different sets of computations when faced with increasingly noisy stimuli was recently demonstrated for circuitries that compute direction selectivity (see section “FEATURE COMPUTATION”; Chen et al., 2016).

Feature Computation

It has been more than a century since Santiago Ramon y Cajal suggested complex signal flow in the retina merely based on the tissue's complex anatomical organization (Cajal, 1893). Starting with just a handful of neuron types in the outer retina, the network generates a wealth of diverse, parallel signal streams first at the level of the BCs and then once again at the level of the ACs and RGCs. Between these levels, the signal flow is dominantly feed-forward, which dictates that any visual feature selected for by downstream retinal neurons must already be present, albeit buried among other features, in their upstream synaptic elements. This means that early visual neurons need to adopt more broadband properties than late-stage neurons.

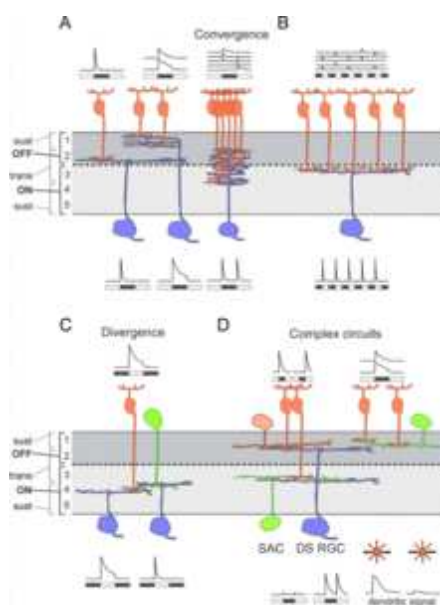
A typical photoreceptor is rather unselective to the nature of the visual input—as long as the rate of photons of the appropriate wavelength range bombarding its outer segment varies over time, the cell will respond with a change in membrane potential (within limits, as discussed in “OVERVIEW”). This contrasts with most RGC types, which often respond only weakly or not at all to a coarse perturbation in the input such as a change in overall brightness, unless this perturbation in addition carries a specific spatial, temporal, and/or chromatic structure (Lettinger et al., 1959). Here, one example is the group of so-called directionally selective (DS) RGCs (Barlow et al., 1964), which respond only weakly to a full-field change in brightness. Instead, DS RGCs respond vigorously when an object moves across the retinal surface in one specific direction but not at all when the same object moves in the opposite direction (Barlow & Hill, 1963, Borst & Euler, 2011). Some types of DS RGCs are tuned to global shifts, others to small moving objects independent of their contrast. Moreover, depending on the species—and thus, eye-size—the details of the circuit can be different (Ding et al., 2016). In all cases, however, the neuronal circuit generating the specific feature tuning of DS RGC takes the original broadband responses of many photoreceptors and passes them through a series of processing stages to ultimately build a visual motion detector. To better understand how this and other computations can be implemented by the circuit connecting photoreceptors and RGCs requires a closer look at number of key computational motifs.

A hallmark of retinal processing is that neurons specifically responding a certain visual feature are usually complemented by a set of neurons that are suppressed by the very same feature. For instance, vertebrate photoreceptors hyperpolarise as light levels increase, whereas only about a third of the BC types does so; the remaining two thirds depolarizes instead (Werblin & Dowling, 1969). This dichotomy is created at the photoreceptor-BC synapse, as different BC types express different combinations of postsynaptic glutamate receptors on their dendrites. Thus, they can be allowed to specifically shape their postsynaptic responses given a common input (DeVries & Schwartz, 1999; DeVries, 2000; Puller et al., 2013). In mammals, BCs that depolarize to a decrease in light (OFF) express “standard” ionotropic glutamate receptors, which become permeable for cations upon glutamate binding, thus depolarizing the cell in the dark when glutamate release from photoreceptors is maximal. As such, the synaptic connection from photoreceptors to OFF BCs is “sign-conserving,” meaning increased photoreceptor activity leads to increased OFF BC activity. In contrast, BCs that depolarized to an increase in light (ON) express a metabotropic glutamate receptor (mGluR6) on their dendrites (Nakajima et al., 1993; Akazawa et al., 1994). This receptor is inversely coupled to cation channels via an intracellular signaling cascade, such that it closes the channels upon glutamate binding (Shen et al., 2009). ON BCs therefore depolarize in the light when glutamate release from photoreceptors is minimal.

The set of photoreceptors typically contacted by BC types differs in number, photoreceptor subclass (rod vs. cone) and spectral sensitivity (Li et al., 2012; Wässle et al., 2009; Behrens et al., 2016). The most prominent example is here the so-called blue-cone BC (cone BC type 9 in mouse), which is present in all mammals studied to date. It exclusively contacts short wavelength-sensitive (S) cones and avoids all other cone types (Haverkamp et al., 2005), thus it represents a chromatically selective (“blue”) channel. In contrast, most other cone BCs make non-

selective cone contacts (as well as rod contacts in some cases) and thus represent achromatic visual channels (Breuninger et al., 2011). Finally, rod BCs (or “mixed” BCs in fish) greatly prefer rods over cones, thus giving rise to the main inner retinal pathway for vision under dim light (scotopic vision) (Sharpe & Stockman, 1999). Together, BCs therefore take the photoreceptor input and break it into several parallel representations, each distinct and more selective than the original input (Wassle, 2004, Euler et al., 2014).

Next, the feature representation of the BC channels is systematically sent to different depths of the IPL, forming distinct functional strata (Figure 4). Classically, the mammalian IPL is divided into five strata, with OFF BCs stratifying in the first two (indexed from the inner nuclear layer side) and ON BCs including rod BCs stratifying in strata three to five. Here, BCs, which are glutamatergic, provide the main excitatory drive. Their axon terminals interact with the processes of ACs and in parallel forward their output to the dendrites of RGCs. This synaptic locus is probably the most powerful computational element of the retina—at the same time, it is the least understood, largely owing to our still rudimentary functional understanding of the diversity in AC types and their circuits.



Click to view larger

Figure 4. Inner retinal circuit motifs. A, the inner plexiform layer (IPL) of the retina is organized into multiple strata each harbor the processes of neurons with distinct response properties. For example, mouse “sustained” and “transient” OFF cells of the mouse tend to stratify in IPL stratum 1 and 2, respectively. Some inner retinal neurons occupy multiple strata and therefore inherit a combination of response properties. B, pooling across several neurons, each with a low response probability but high temporal precision, can result in an output that is both precise and reliable (Baden et al., 2011). C, different postsynaptic circuits emanating from the same bipolar cell may inherit different response properties under the control of, for example, amacrine cells (Asari & Meister, 2014). D, differential combination of bipolar cell inputs with different temporal response properties on different parts of the postsynaptic dendrite could give rise to directionally

Typically, spatial receptive fields (RFs) of BCs feature an antagonistic center-surround structure, with a strong surround component that renders BC responses sensitive to stimulus size (Kuffler, 1953, Eggers et al., 2007; Franke et al., 2016). The RF center component is largely driven by dendritic inputs in the outer retina, whereas the surround component reflects the combined input received from the HC networks in the OPL, as well as from several BC-AC circuits feeding onto the BC’s axon terminals. The latter circuits may be direct, for example, involving but a single type of AC that is driven by the BC itself (reciprocal feedback, Hartveit, 1997; Chávez et al., 2006) or by other BC types. However, also more complex circuits can be found that involve several serial connections amongst distinct types of ACs as well as other BCs (e.g., Eggers & Lukasiewicz, 2011; Eggers et al., 2007). Consequently, the functional diversity between BC channels is only partially established in the OPL; the IPL offers a lot of extra hardware for sophisticated computations. For example, the functional heterogeneity between BC types markedly increases as their AC-based surround is being recruited using larger stimuli (Franke et al., 2016).

While the nuanced functional role of most ACs remains elusive, a small number of BC-AC circuits have been studied at substantial depth (Masland, 2012; MacNeil & Masland, 1998; Eggers et al., 2007; Eggers & Lukasiewicz, 2011). These include, as the “central element,” AII (Bloomfield & Dacheux, 2001), A17

tuned responses (Kim et al., 2014). Schematics adapted from Euler et al. (2014).

(Grimes et al., 2010; Nelson & Kolb, 1985) and starburst amacrine cells (Euler et al., 2002; Famiglietti Jr., 1983; Masland, 2005). In all cases, the studied ACs

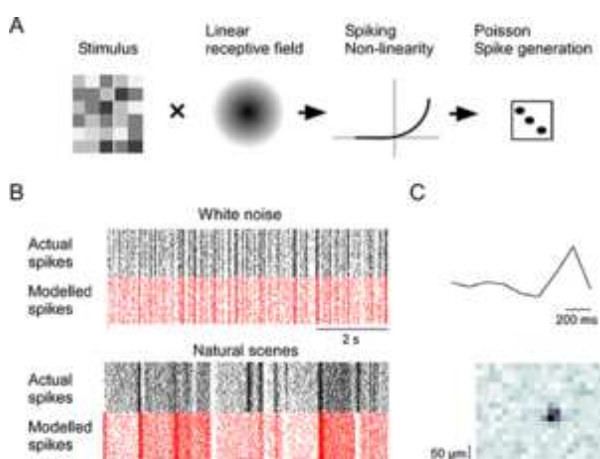
play different and quite distinct functional roles in one or often multiple circuits and with their dendrites acting as both input and output sites. A recent example is the vGluT3-expressing AC, which uses glycine and glutamate as transmitters (Haverkamp & Wässle, 2004). This so-called glutamatergic AC (GAC) broadly stratifies in the centre of the IPL and receives input from both ON and OFF BCs. GACs are involved in at least four circuits (Lee et al., 2014; Tien et al., 2016; Lee et al., 2016): They provide (1) glycinergic inhibition to RGCs that are suppressed by contrast (“uniformity detectors”), and glutamatergic excitation (2) to direction-selective RGCs, (3) OFF alpha RGCs, which are highly contrast-sensitive, and (4) W3 RGCs, which are sensitive to local motion of any direction. These different functional roles of GAC synaptic output are made possible by functional segregation within the cell’s dendritic arbor (Tien et al., 2016; Lee et al., 2016). Whether the different GAC “functions” are active in parallel or selectively triggered by specific visual stimulus properties is not completely understood. At least one other type of AC was shown to “switch function” depending on the stimulus condition: at low light levels, All ACs are the central hub of the primary rod pathway, while at higher light levels, they are involved in the detection of an approaching object (“looming detectors,” discussed in Munch et al., 2009).

Finally, RGCs typically integrate across often several dozens to hundreds of retinal interneurons; their dendritic arbors ramify in one or multiple specific strata of the IPL to receive synaptic from distinct subsets of BC and AC types (Roska & Werblin, 2001). This highly selective connectivity is the main basis of the functional diversity among RGC types. Accordingly, RGCs that stratify in the “OFF portion” of the IPL tend to exhibit OFF responses, those with their dendrites in the IPL’s ON portion ON responses (Figure 4A). Similarly, the spatial extent of an RGC’s dendrites across the retinal surface is highly predictive about the size of its RF centre and thus the spatial resolution of a RGC channel (Nelson & Kolb, 1983). In primates, foveal “midget-type” RGCs pick up synaptic drive from a single (midget) BC, which in turn connects to a single cone—thus forming the channel with the highest possible resolution (Kolb & Marshak, 2003). In contrast, primate parasol cells integrate across many dozens neighboring BCs and thus hundreds of cones (Field et al., 2010) to form a low spatial resolution channel. Other RGCs that integrate across multiple IPL strata refine their response properties by “mixing” diverse inhibitory and excitatory synaptic inputs (Sivyer et al., 2010). More dramatically, some RGCs connect spatially asymmetrically to their presynaptic partners. The most prominent example here is the aforementioned group of direction-selective RGCs, which has been found in many mammals (except primates so far) (Borst & Euler, 2011; Vaney et al., 2012): They only connect starburst amacrine cells (SACs, Famiglietti, 1983) located on one side of the RGC (Briggman et al., 2011). Since SACs provide directionally tuned inhibitory inputs, they prevent the DS RGCs from responding to stimuli moving into the RGC’s RF from the SAC side, thereby tuning the RGC’s response preference to the opposite direction. Such asymmetrical connectivity is not reserved for RGCs: For example, the concentric distribution of inputs that SACs receive from BCs and ACs along their dendrites is also asymmetrical, an arrangement that may contribute to DS in SACs (Ding et al., 2016; Greene et al., 2016; Kim et al., 2014) (Figure 4D).

The specific synaptic organization of the different RGC circuits and the cellular properties of the circuit elements results in the observed high functional diversity of RGC channels to the brain (Gollisch & Meister, 2009). Like for the BCs, visual feature selectivity is often organized antagonistically in RGCs, with light-step polarity (ON vs. OFF) being the simplest one. Other, more complex examples include contrast sensitivity (e.g., alpha RGCs; see Schwartz et al., 2012), which are most sensitive to contrast vs. the group of “suppressed-by-contrast” (SBC) RGCs (Tien et al., 2015).

The cellular nuances of different circuits aside, how can one more formally describe and study retinal function? Clearly, a unified language is required. For example, can one concoct a series of equations, given that the appropriate values for each variable are substituted, capture the functional “essence” of any one cell or channel?

A first step toward this goal is the Linear-Nonlinear-Poisson (LNP) model (Chichilnisky, 2001; Baccus & Meister, 2002) (Figure 5A, Figure 5B). Here, the response properties of a neuron are captured by a linear filtering operation followed by a nonlinearity, assuming that spikes are generated by a Poisson process with the rate determined by the nonlinearly transformed filter output. The linear filter provides an approximation of the neuron’s RF in space and time, while the nonlinearity maps this filter’s output to spike rate, accounting for the typical threshold linear responses of many cells. Classically, a “noise” stimulus is presented and the neuron’s output measured. Then, the neuron’s response is reverse-correlated to the stimulus: Whenever the neuron responds, this operation looks at the stimulus that just preceded this response and performs an average of this stimulus (“spike-triggered average”) (Figure 5C). The result is an estimate of the stimulus that optimally activated the neuron. Next, the stimulus can be convolved with the linear filter to yield a prediction of how the neuron would have responded if there was no additional rectifying nonlinear operation. The difference between the result of this convolution and the actual response of the neuron reflects the (spiking) nonlinearity. For fine-tuning, additional terms modeling spike refractory periods or bursting behavior can also be integrated (Pillow et al., 2008).



Click to view larger

Figure 5. Modeling retinal response properties. A, illustration of the standard linear-nonlinear-Poisson model (LNP), where a stimulus is processed by a linear filter before it is passed through a nonlinearity. The spiking response is then generated through a random process. B, measured and predicted spikes to white noise stimulus (top, like in A) and natural scenes (bottom) for a primate RGC (from Heitman et al., 2016). C, temporal (top) and spatial (bottom) components of a receptive field of a mouse bipolar cell.

Several extensions and modifications of the LNP model have been put forward (for an overview, see, e.g., Schwartz et al., 2006 and Real et al., 2017), each offering solutions to more closely describe a neuron’s functional properties. The most straightforward extension replaces the single linear filter by a series of filters, whose output is not simply rectified but squared, for example. In this case, the filters can be obtained using a technique called “spike-triggered” covariance (Aljadeff et al., 2016; Fairhall et al., 2006). More recent extensions break the linear receptive field into several subfields, each with its own nonlinearity (McFarland et al., 2013; Freeman et al., 2015). Similarly, a cascade of LN-models with feedback terms inspired by retinal anatomy has recently been suggested (Real et al., 2017). Also, these models allow for an anatomical interpretation of the inferred subunits: cancellation experiments in midget RGCs suggest that the subunits indeed correspond to the signal derived from single BCs (Freeman et al., 2015; Schwartz et al., 2012).

The basic LNP model often captures a large fraction of a neuron’s response variance to simple stimuli for certain cell types (up to 85% for ON and OFF parasol RGCs in the macaque, [Heitman et al., 2016]). However, for many cell types, simple LNP models are insufficient. For instance, it typically will not accurately capture responses of inherently nonlinear cell types. In addition, responses to more complex stimuli, such as natural movies, are typically not described well by the basic LNP model (Heitman et al., 2016) (Figure 5B).

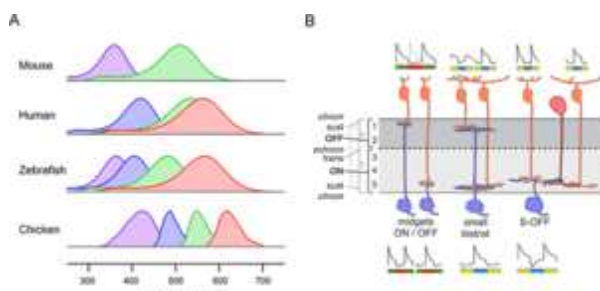
Several extensions and modifications of the LNP model have been put forward (for an overview, see, e.g., Schwartz et al., 2006 and Real et al., 2017), each offering solutions to more closely describe a neuron’s functional properties. The most straightforward extension replaces the single linear filter by a series of filters, whose output is not simply rectified but squared, for example. In this case, the filters can be obtained using a technique called “spike-triggered” covariance (Aljadeff et al., 2016; Fairhall et al., 2006). More recent extensions break the linear receptive field into several subfields, each with its own nonlinearity (McFarland et al., 2013; Freeman et al., 2015). Similarly, a cascade of LN-models with feedback terms inspired by retinal anatomy has recently been suggested (Real et al., 2017). Also, these models allow for an anatomical interpretation of the inferred subunits: cancellation experiments in midget RGCs suggest that the subunits indeed correspond to the signal derived from single BCs (Freeman et al., 2015; Schwartz et al., 2012).

Functional models so far have only been used to provide compact descriptions for a handful of cell types and comprehensive models accounting for the full diversity of RGC signalling and the associated circuits have been lacking. Recent advances in experimental techniques, such as population recordings (Field et al., 2010; Baden et al., 2016; Franke et al., 2016), single-cell transcriptomics (Shekhar et al., 2016) and large-scale EM reconstructions (Ding et al., 2016; Briggman et al., 2011) suggest that a wealth of information on responses to complex stimuli, the complement of active membrane components and detailed circuit diagram, respectively, will become available in the near future and accelerate building better models toward a comprehensive understanding of RGC computations.

Circuits for Color Vision

“Color” is a perception that arises at higher visual processing levels but relies heavily on chromatic pathways that originate in the retina (Dacey & Packer, 2003; Dacey, 2000; Neitz & Neitz, 2011). For an animal to distinguish, say, a blueberry from the surrounding leaves, it cannot rely on brightness differences alone, as those depend on illumination. For example, the spectrum of daylight changes over the course of a day: Mornings and evenings are more long-wavelength biased (red) compared to the more short-wavelength-(blue)-biased midday sun. The visual system exploits differences in the light spectrum of objects, and this ability is referred to as “color vision.” The spectrum of the light emanating from an object is determined by several factors, including the illumination spectrum, the object’s spectral reflectance and potentially also its transmission and/or emission spectrum. For inferring “color” of an object (~its reflectance), the visual system therefore also needs to take account of the context into which the object is embedded. The result is a color perception that is largely independent of illumination conditions (“color constancy”; see Kelber et al., 2003; Foster, 2011; Krauskopf et al., 1982; Hurvich & Jameson, 1957).

Photoreceptors are oblivious to colors; they translate light of different wavelengths into levels of brightness as a function of their opsin’s spectral sensitivity. Therefore, to differentially probe the spectrum of light, at least two types of photoreceptors with opsins of different spectral sensitivity are needed as the minimum retinal requirement for color vision. Usually two or more types of cone photoreceptors are involved—as they come in different spectral flavors (Figure 6)—but also the different spectral sensitivities between rods and cones have been implicated with color vision under certain light levels in some animals including humans (Joesch & Meister, 2016; Reitner et al., 1991; Field et al., 2009). At the extreme end, some amphibians feature two types of spectrally distinct rods that may also support some form of color vision (Hailman, 1976; Korenyak & Govardovskii, 2013; Denton & Wyllie, 1955).



[Click to view larger](#)

Figure 6. Color vision. A, exemplary action spectra of

Color vision is generally widespread among vertebrates (Peichl, 2005; Jacobs & Rowe, 2004), and most of them feature at least two spectral cone types: one sensitive to short wavelengths (S-cone, “blue” or “UV”) and a second one sensitive to longer (“medium”) wavelengths (M-cone, “green”). A few vertebrates, including whales, dolphins, and many sharks, and racoons, feature just one cone type (Griebel & Peichl, 2003; Von Schantz et al., 1997). These animals are “monochromats” and, thus,

different vertebrates' cone complements. B, inner retinal circuit motifs for chromatic processing. Midget ganglion cells of the primate fovea are excited by a single L- or M-cone and received inhibited over a wider area. They therefore inherit a “pure” L- or M-center and a mixed surround. Small bistratified ganglion cells pool across blue (S-cone) ON and yellow (M- +L-cone) OFF bipolar cells to yield blue^{ON}-yellow^{OFF} responses. Other RGCs receive differential chromatic information through an amacrine cell. Schematic in B adapted from (Euler et al., 2014).

these primates are “color specialists” amongst *synapsida* (proto-mammals), their abilities are typically superseded by shallow water fish and *sauropsida*. Many birds and reptiles possess four or even five spectral cone types and are thus “tetrachromats” or “pentachromats,” respectively (Figure 6A). For comparison, many visually oriented invertebrates are at least tetrachromats (Jacobs & Rowe, 2004; Kelber et al., 2003), with mantis shrimp at the lead with a total of 12 spectral photoreceptor types (Thoen et al., 2014). However, to what extent most of these animals use their more diverse photoreceptor complements is not completely understood. While it is clear that some animals, such as many turtles and teleost fish, feature complex chromatic responses in retinal neurons (e.g., Haverkamp et al., 1997, Ammermueller et al., 1995), it remains unclear if these signals are a dominant aspect of these animal's retinal output.

As discussed above, color vision requires information about the spectrum of the incoming light. Hence, the signals of the different cone types—basically read-outs of two or more (partially overlapping) spectral bands—need to be combined by downstream circuits in a fashion that preserves spectral information. The retinal strategy for this is “color opponency” (Hurvich & Jameson, 1957; Krauskopf et al., 1982); to compute the difference between pairs of spectrally distinct cone channels (or one cone channel versus the sum of two others), resulting, for example, in an output signal that is excited by “blue” and inhibited by “yellow” light (blue^{ON}-yellow^{OFF}) (Calkins et al., 1998; Chichilnisky & Baylor, 1999; Dacey, 2000) (Figure 6B). Such a color-opponent signal may be viewed as a “minimalistic” representation of a light spectrum. Color opponency can be implemented at different retinal levels employing different sets of neuron types. Here, probably the best-studied example is the circuit of the so-called “small bistratified” (SB) RGC in the primate retina (Dacey & Lee, 1994; Crook et al., 2009; Zrenner & Gouras, 1981; Calkins et al., 1998). The dendritic arbor of this RGC type taps into two strata of the IPL to receive excitatory input from ON BCs that selectively contact S-cones (“blue-cone ON BCs”) as well as excitatory input from OFF BCs that likely avoid S-cones but mainly contact M- and L-cones (Ghosh & Grünert, 1999). As a result, this RGC spikes vigorously in the presence of blue light (mediated by S-cones) or in the absence of yellow light (mediated by M- + L-cones). Beside the SB cell, at least two further primate RGC types feature some form of blue-yellow opponency albeit with different polarity and/or RF size (Dacey, 2000).

All mammals studied so far feature relatively similar circuits that generate short versus longer wavelength opponent output; due to the lack of the L-opsin in non-primate mammals they are referred to as “blue-green” rather than “blue-yellow” (Puller et al., 2011). However, also multiple types of chromatically opponent RGCs usually exist here, as was shown, for instance, in guinea pigs (Yin et al., 2009), rabbits (Mills et al., 2014), and ground squirrels (Sher & DeVries, 2012). These RGC types often include both blue^{ON}-green^{OFF} and blue^{OFF}-green^{ON} versions. The circuit underlying blue^{OFF}-green^{ON} opponency typically involves a monostratified RGC with its dendrites ramifying in the IPL's ON sublayer: The cell receives its blue^{OFF} component indirectly from S-cone ON BCs via an inhibitory AC that sign-inverts the BC input (Chen & Li, 2012), whereas the green^{ON} signal is

expected to be “color blind” (but see above). Most terrestrial mammals are “dichromats,” which feature two spectral cone types: an S-cone and an M-cone (Szél et al., 1992; Jacobs, 1993; Neitz & Neitz, 2011). Among mammals, only a subset of primates—old-world monkeys and the great apes, including humans—are “trichromats”: due to an evolutionary “recent” gene duplication event, they possess an additional cone type with a red-shifted opsin sensitive to longer-still wavelengths (L-cone, “red”) (Nathans, 1999). While

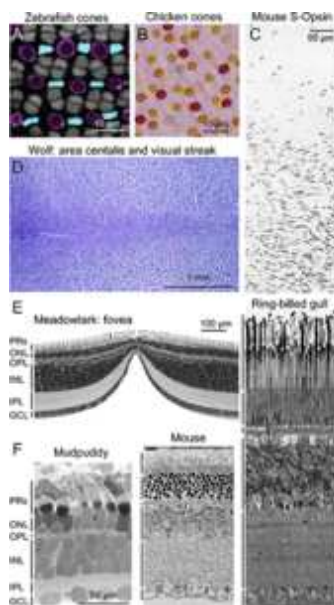
provided directly either by ON BCs that are M-cone selective or that contact all cones within their reach. The latter is possible because the S-cone density is usually much lower than the M(L)-cone density (Peichl, 2005) and, hence, even cone non-selective BCs carry a strongly green-dominant signal (Breuninger et al., 2011; Behrens et al., 2016). This may be the reason why the S-cone ON BC, which is highly conserved across mammalian species (Haverkamp et al., 2005; Li & DeVries, 2004; Mariani, 1984; Kouyama & Marshak, 1992), appears to have no consistent chromatic “counterpart”: for example, mice feature an abundant M-cone OFF BC type (Breuninger et al., 2011; Behrens et al., 2016), whereas in rabbits it appears to be scarce (Mills et al., 2014). Both species appear to lack an M-cone ON BC type, whereas ground squirrels possess both ON and OFF variants of M-cone BCs (Li & DeVries, 2006). Note that also interactions in the outer retina (i.e., HC feedback to cones, may be play a role in color opponency). In primates, for instance, color opponency was already demonstrated at the level of the S-cones, with the blue RF center being antagonized by a yellow RF surround provided by a specific HC type (Packer et al., 2010). HCs have also been implicated in color opponency in the rabbit retina (Mills et al., 2014). Moreover, chromatic processing by the OPL appears to be much more prominent in many non-mammalian vertebrates (Ventura et al., 2001; Kamermans et al., 1991).

The “recent” appearance of the L-cone in many primates gave rise to another color axis—“green” vs. “red” (roughly M- vs. L-cones, see later in this section) (Nathans, 1999). While blue-yellow (blue-green) opponency is thought to originate from evolutionary old, highly conserved retinal circuits (see earlier in this section), primate red-green opponency is considered largely a “by-product” of the midget pathway, the primate’s high-spatial acuity system (Field et al., 2010; Jusuf et al., 2006). In the fovea, the 1:1:1 connectivity between cone, midget BC and midget RGC (Kolb & Marshak, 2003) yields ON and OFF RGCs with chromatically pure green (M-cone) or red (L-cone) RF centers “by design.” The antagonistic RF surround is thought to average over the neighboring cones (Lee, 1996) and, therefore, resulting in four basic types of opponency: $M^{ON}-(M+L)^{OFF}$, $M^{OFF}-(M+L)^{ON}$, $L^{ON}-(M+L)^{OFF}$ and $L^{OFF}-(M+L)^{ON}$. Note that this RF organization is different from that of the SB RGCs, where color opponency is not a consequence of center-surround RF interactions; their RF center is readily blue^{ON}-yellow^{OFF} color opponent.

The circuit providing the chromatically antagonistic surround in midget cells is not yet entirely clear. Some evidence points to the involvement of HCs, which establish the surround already at the cone level (Verweij et al., 2003) and render both cone and midget BC color opponent (Crook et al., 2011). However, a contribution of ACs for setting up the midget surround (i.e., outside the fovea) remains a possibility (Dacey et al., 2000). How the midget system works outside the fovea, where midget BCs contact multiple cones and midget RGCs multiple BCs, is also not completely understood. The finding that color opponency in midget RGCs does not substantially decline toward the retina peripheral (Martin et al., 2001) suggests the existence of mechanisms that preserves some (opposite) chromatic predominance in RF center versus RF surround. Such a chromatic predominance may be introduced by a bias in the cone type-connectivity of midget BCs (Field et al., 2010) and/or by sampling an irregular cone mosaic with elongated RGC dendritic fields (Martin et al., 2001).

In contrast to many non-mammalian species, in which the different cone types are arranged in regular, almost crystalline mosaics (e.g., in many fish [see Salbreux et al., 2012] and birds [Kram et al., 2010]) (Figure 7A, 7B), mammals possess highly irregular (“clumpy”) cone mosaics with clusters of the same cone types [see Roorda & Williams, 1999]). Such “clumpy” cone distributions and/or more global anisotropies in the cone mosaic (i.e., opsin expression gradients; see Röhlich et al., 1994), in combination with non-selective sampling alone, can generate some chromatic antagonism in RGC that are commonly not considered to take part in chromatic processing (discussed in Chang et al., 2013). Here, an intriguing example is the emergence of red-green opponency (and

trichromacy) in transgenic mice after introduction of the human L-opsin (Jacobs et al., 2007; Smallwood et al., 2003; but see Makous, 2007).



Click to view larger

Figure 7. Retinal specializations. A, the crystalline cone-lattice of zebrafish features exactly twice as many L- and M-cones (gray) compared to blue and UV S-cones (colored) (adapted from Fraser et al. (2013). B, in contrast, the cone-mosaics of each cone type in chickens is independent of the other cones (adapted from (Kram et al., 2010). C, Mouse cones feature a prominent ventral to dorsal S-opsin gradient across the retina (adapted from Haverkamp et al., 2005). D, retinal ganglion cells of the wolf retina exhibit dramatically increased densities in the area centralis (left) and along a visual streak aligned with the visual horizon (vertical center) (adapted from Peichl, 1992). E, many birds, such as the meadowlark, feature one or multiple foveae where most retinal neurons are pushed to the side to allow more direct access of light to a particularly high density of cones (adapted from (Tyrrell et al., 2013). F, retinal cross-sections of different vertebrates highlight dramatic differences in retinal thickness and complexity (image of mudpuppy retina kindly provided by Leo Peichl; mouse and gull were taken from (Williams et al., 1998) and (Emond et al., 2006), respectively. Scale-bar in F reflects all three panels).

(e.g., Baden et al., 2013). The other group of animals, the old-world primates including humans, are trichromats; but they are perhaps rather peculiar ones, as this trichromacy arose recently in evolution. Much of the additional spectral information made available by the gene duplication of M/L-opsin appears to be harnessed not by the retina but by the cortex—and by mechanisms that are far from understood. This focus on “mice and men” has largely left color vision by most vertebrates out of the bargain. For example, how does a retina deal with the complexity arising from four or more spectral cone inputs? Retinal organization of tetra- or pentachromatic animals such as many reptiles, birds, and surface-dwelling fishes tends to be substantially more complex than that of mice or

It is important to emphasize that chromatic processing by retinal pathways is only the first step toward color perception. In fact, our knowledge of those pathways is disturbingly incomplete, as important psychophysical observations cannot be satisfyingly explained by any of the circuits described above (for discussion, see Neitz & Neitz, 2011; Lee et al., 2010). For instance, no substantial deficits in blue-yellow vision were detected in humans with a function-loss mutation in the gene coding for the glutamate receptor that mediates photoreceptor transmission to ON BCs—including the S-cone ON BC (Dryja et al., 2005). Furthermore, a recent psychophysics study revealed an unexpected heterogeneity in the color perception evoked by the stimulation of individual, spectrally identified cones located near the fovea (Sabesan et al., 2016): other than expected from the “midget theory,” M- and L-cones evoked not only red or green but also white (achromatic) percepts. In addition, a cone whose neighborhood was dominated by cones of opposite spectral identity—an arrangement that should optimally trigger a center-surround based mechanism of color opponency—did not necessarily relay a more robust color percept.

Looking across current knowledge on vertebrate retinal circuits for color vision, one cannot help but notice that most work has been done in two groups of animals that perhaps have the least representative circuits for color vision in the animal kingdom. The dichromatic mouse, though broadly representative for many terrestrial mammals, is not a color specialist and over evolutionary time has adjusted some of its circuits for color vision to subservise functions not primarily concerned with discriminating wavelength independent of intensity

primates (Figure 7). Is this complexity a direct consequence of the need to compute more spectral information? The few available studies on some of these retinas reveal a staggering diversity in the way that different retinal neurons are tuned to wavelength, with chromatic computations of retinal neurons ranging from simple “long- vs. short-wavelength” opponency as seen also in mice and primates, to a broad range of “sandwich-type” opponencies (e.g., with long- plus short- versus mid-wavelengths). Which chromatic computations predominate in these retinas, and how are they implemented by circuits in the outer and inner retina?

Environmental Adaptations

While the main retinal cell classes and their general connectivity rules are heavily conserved between vertebrates, each species nonetheless comes with its own peculiarities geared to optimize their visual apparatus to their specific visual habitat (Land & Nilson, 2012; Cronin et al., 2014). For example, predominantly nocturnal animals tend to have a rod-dominated retina embedded in larger eyes, whereas diurnal species tend to feature a larger fraction of cones (Peichl et al., 2000). In addition, most large mammals—such as dogs, cats, or deer but also marine mammals—feature a “mirror” in the back of the eye, called tapetum lucidum (Lee, 1886). This simple trick increases the retina’s light sensitivity by effectively doubling a photon’s chance to hit an opsin as it traverses the photoreceptor outer segments for a second time. Following the no-free-lunch principle, the downside is some inevitable image blur. To avoid “blinding themselves” during the day, tapeta of many animals are restricted to the dorsal part of the eye, thus avoiding reflection of direct sunlight from above (Ollivier et al., 2004).

Next, some species—such as primates, as well as many reptiles and birds—feature one or more fovea(s) to support high spatial acuity vision (Fite & Rosenfield-Wessels, 1975) (Figure 7E). In contrast, the retina of animals that rely heavily on scanning the visual horizon, such as rabbits or dogfish, often possess a so-called visual streak—an increased neuron density aligned with the horizon (Peichl, 1992) (Figure 7D). In some cases, such specializations can be extreme. One example is *Anabplebs*, the “four eyed fish”; it lingers at the water surface with half of each eye submerged, thus simultaneously monitoring the visual world above and below the water surface. The entire eyeball including retina has adapted to the two environments in such a dramatic manner that it appears like the animal has two separate eyes on each side of the head (Sivak, 1976; Owens et al., 2009; Swamynathan et al., 2003). Clearly, visual systems will use every trick conceivable to better match their response properties to the statistics of their natural input.

But most adaptations are more subtle. For example, mice (as well as rats and even hyenas) feature a dorsal-ventral opsin gradient (Applebury et al., 2000; Baden et al., 2013; Szél & Roehlich, 1992) (Figure 7C). Only M-cones in the dorsal part of the retina exclusively express M-opsin, while toward the ventral edge the same cone type progressively co-expresses S-opsin. As such, the retina’s sensitivity to short-wavelength light increases with increased visual elevation, a feature that has traditionally been linked to the differential distribution of wavelengths above and below the visual horizon. However, at least in mice, this gradient serves a second function: in addition to preferentially responding to blue/UV light, ventral co-expressing cones also respond more non-linearly than “pure” dorsal M-cones (Baden et al., 2013) and thus preferentially respond to dark stimuli on a bright background. This nonlinearity correlates with an increased preponderance of dark contrasts above the horizon, driven by overhanging vegetation or the presence of the silhouette of an aerial predator against the bright backdrop of the daylight sky.

Other retinal neurons can also vary with location. Many do not homogeneously cover the retinal surface but feature

distinct densities in specific regions. For example, the so-called W3 RGC, which represent the “local edge detector” (LED) cells of the mouse and favors small moving black objects, has its highest density in the center of the ventral retina (Zhang et al., 2012). Even neurons of a single type that as a population do cover the entire retinal surface can change their response properties or the specifics of their computations with retinal position. One example is the genetically identified JAM-B RGC, which changes the shape of its dendritic arbor from asymmetrical to concentric as a function of position along the dorso-ventral axis. Consequently, JAM-B RGCs are DS in the dorsal retina (Kim et al., 2008) but not in the ventral retina, where they display color opponent responses (Joesch & Meister, 2016).

Finally, retinal complexity differs dramatically between species. For example, the retina of birds is often nearly twice as thick as that of rodents (Emond et al., 2006) (Figure 7F), likely reflecting a great number of additional neurons, potentially required to deal with their specific visual requirements. On the other extreme end, the retina of mudpuppies is thin and harbors substantially fewer, albeit larger neurons (Figure 7F). In addition, different species appear to “relocate their computational arsenal” depending on how much further computation will be carried out in the brain: Several computations pinned to RGC circuits in rodents or lagomorphs (e.g., rabbits), such as orientation selectivity or contrast-suppression are already a feature of the BC output in fish (Antinucci et al., 2016; Rosa et al., 2016). Conversely, primates appear to lack directional-selective RGCs, which represent a substantial fraction of the RGCs of most non-primate mammals studied to date (Nikolaou et al., 2012; Vaney et al., 2012). Perhaps primates moved these essential computations to the cortex? In support of this notion, the largest fraction of RGCs in the primate retina are midget cells and serve the foveal high-acuity system. Moreover, the midget RGC’s circuit appears to be rather simple, potentially reflecting the “relocation” of processing hardware to downstream visual areas in the cortex.

Taken together, the many differences and specializations seen across species or across retinal position within a species highlight a highly dynamic and purpose-built view of retinal processing. Vision is a pivotal sense for many animals, and it is energetically expensive. Accordingly, modifications or tricks that optimize the visual system’s performance for a given set of tasks can evolve rapidly and repeatedly from a common retinal blueprint as animals explore new visual niches (Land & Nilson, 2012; Cronin et al., 2014). In the future, it will be exciting to more broadly study the types of specializations that different retinas have come up with in the context of their visuo-ecological purpose and to study how retinas change over evolutionary time scales to accommodate new visual requirements.

Acknowledgments

We would like to thank Anton Nikolaev for his helpful discussions. This work was supported by funding from the European Commission (ERC-StG NeuroVisEco 677687 to T.B.), the Deutsche Forschungs-gemeinschaft (DFG; EXC307 to T.E., SCHU 2243/3-1 to T.S.; BE5601/1-1 to P.B., and BA5283/1-1 to T.B.), and the Bernstein Centre for Computational Neuroscience (01GQ1601 to P.B.).

References

Akazawa, C., Ohishi, H., Nakajima, Y., Okamoto, N., Shigemoto, R., Nakanishi, S., & Mizuno, N. (1994). Expression of mRNAs of l-AP4-sensitive metabotropic glutamate receptors (mGluR4, mGluR6, mGluR7) in the

rat retina. *Neuroscience Letters*, 171(1–2), 52–54.

Find this resource:

Ala-Laurila, P., Greschner, M., Chichilnisky, E. J., & Rieke, F. (2011). Cone photoreceptor contributions to noise and correlations in the retinal output. *Nature Neuroscience*, 14(10), 1309–1316.

Find this resource:

Aljadeff, J., Lansdell, B. J., Fairhall, A. L., & Kleinfeld, D. (2016). Analysis of neuronal spike trains, deconstructed. *Neuron*, 91(2), 221–259.

Find this resource:

Ammermüller, J., Müller, J. F., & Kolb, H. (1995). The organization of the turtle inner retina. II. Analysis of color-coded and directionally selective cells. *The Journal of Comparative Neurology*, 358(1), 35–62.

Find this resource:

Angueyra, J. M., & Rieke, F. (2013). Origin and effect of phototransduction noise in primate cone photoreceptors. *Nature Neuroscience*, 16(11), 1692–1700.

Find this resource:

Antinucci, P., Suleyman, O., Monfries, C., & Hindges, R. (2016). Neural mechanisms generating orientation selectivity in the retina. *Current Biology*, 26(14), 1802–1815.

Find this resource:

Applebury, M. L., Antoch, M. P., Baxter, L. C., Chun, L. L. Y., Falk, J. D., Farhangfar, F., ... Robbins, J. T. (2000). The Murine cone photoreceptor: A single cone type expresses both S and M opsins with retinal spatial patterning. *Neuron*, 27(3), 513–523.

Find this resource:

Arai, I., Tanaka, M., & Tachibana, M. (2010). Active roles of electrically coupled bipolar cell network in the adult retina. *The Journal of Neuroscience*, 30(27), 9260–9270.

Find this resource:

Arshavsky, V. Y., Lamb, T. D., & Pugh, E. N. (2002). G proteins and phototransduction. *Annual Review of Physiology*, 64, 153–157.

Find this resource:

Asari, H., & Meister, M. (2014). The projective field of retinal bipolar cells and its modulation by visual context. *Neuron*, 81(3), 641–652.

Find this resource:

Baccus, S. A., & Meister, M. (2002). Fast and slow contrast adaptation in retinal circuitry. *Neuron*, 36(5), 909–919.

Find this resource:

Baden, T., Esposti, F., Nikolaev, N., & Lagnado, L. (2011). Spikes in retinal bipolar cells phase-lock to visual stimuli with millisecond precision. *Current Biology*, 21(22), 1859–1869.

Find this resource:

Baden, T., Schubert, T., Chang, L., Wei, T., Zaichuk, M., Wissinger, B., & Euler, T. (2013). A tale of two retinal domains: near-optimal sampling of achromatic contrasts in natural scenes through asymmetric photoreceptor distribution. *Neuron*, *80*(5), 1206–1217.

Find this resource:

Baden, T., Nikolaev, A., Esposti, F., Dreosti, E., Odermatt, B., & Lagnado, L. (2014). A synaptic mechanism for temporal filtering of visual signals. *PLoS Biology*, *12*(10), e1001972.

Find this resource:

Baden, T., Berens, P., Franke, K., Roman Roson, M., Bethge, M., & Euler, T. (2016). The functional diversity of retinal ganglion cells in the mouse. *Nature*, *529*(7586), 345–350.

Find this resource:

Baden, T., & Euler, T. (2013). Early vision: Where (some of) the magic happens. *Current Biology*, *23*(24), R1096–R1098.

Find this resource:

Barlow, H. B. (1956). Retinal noise and absolute threshold. *Journal of the Optical Society of America*, *46*(8), 634–639.

Find this resource:

Barlow, H. B., & Hill, R. M. (1963). Selective sensitivity to direction of movement in ganglion cells of the rabbit retina. *Science*, *139*(3553), 412–414.

Find this resource:

Barlow, H. B., Hill, R. M., & Levick, W. R. (1964). Rabbit retinal ganglion cells responding selectively to direction and speed of image motion in the rabbit. *The Journal of Physiology*, *173*, 377–407.

Find this resource:

Barnes, S., Merchant, V., & Mahmud, F. (1993). Modulation of transmission gain by protons at the photoreceptor output synapse. *Proceedings of the National Academy of Sciences USA*, *90*, 10081–10085.

Find this resource:

Baylor, D., Lamb, T., & Yau, K. (1979). The membran current of single rod outer segments. *The Journal of Physiology*, *288*, 589–611.

Find this resource:

Baylor, D. A., Matthews, G., & Yau, K.W. (1980). Two components of electrical dark noise in toad retinal rod outer segments. *The Journal of Physiology*, *309*, 591–621.

Find this resource:

Behrens, C., Schubert, T., Haverkamp, S., Euler, T., & Berens, P. (2016). Connectivity map of bipolar cells and photoreceptors in the mouse retina. *eLife*, *5*, 1206–1217.

Find this resource:

Bloomfield, S. A., & Dacheux, R. F. (2001). Rod vision: Pathways and processing in the mammalian retina. *Progress in Retinal and Eye Research*, *20*(3), 351–384.

Find this resource:

Boelen, M.K., Boelen, M.G., & Marshak, D.W., 1998. Light-stimulated release of dopamine from the primate retina is blocked by L-2-amino-4-phosphonobutyric acid (APB). *Visual Neuroscience*, 15(1), 97–103.

Find this resource:

Borst, A., & Euler, T. (2011). Seeing things in motion: Models, circuits, and mechanisms. *Neuron*, 71(6), 974–994.

Find this resource:

Breuninger, T., Puller, C., Haverkamp, S., Euler, T. (2011). Chromatic bipolar cell pathways in the mouse retina. *The Journal of Neuroscience*, 31(17), 6504–6517.

Find this resource:

Briggman, K. L., Helmstaedter, M., & Denk, W. (2011). Wiring specificity in the direction-selectivity circuit of the retina. *Nature*, 471(7337), 183–188.

Find this resource:

Burkhardt, D. A. (1994). Light adaptation and photopigment bleaching in cone photoreceptors in situ in the retina of the turtle. *The Journal of Neuroscience*, 14(3), 1091–1105.

Find this resource:

Cajal, S. R. (1893). La retine des vertebres. In *The vertebrate retina* (pp. 775–794).

Find this resource:

Calkins, D. J., Tsukamoto, Y., & Sterling, P. (1998). Microcircuitry and mosaic of a blue-yellow ganglion cell in the primate retina. *The Journal of Neuroscience*, 18(9), 3373–3385.

Find this resource:

Chang, L., Breuninger, T., & Euler, T. (2013). Chromatic coding from cone-type unselective circuits in the mouse retina. *Neuron*, 77(3), 559–571.

Find this resource:

Chapot, C. A., Euler, T., & Schubert, T. (2017). How do horizontal cells ‘talk’ to cone photoreceptors? Different levels of complexity at the cone-horizontal cell synapse. *The Journal of Physiology*, 595(16), 5495–5506.

Find this resource:

Chávez, A. E., Singer, J. H., & Diamond, J.S., (2006). Fast neurotransmitter release triggered by Ca influx through AMPA-type glutamate receptors. *Nature*, 443(7112), 705–708.

Find this resource:

Chen, S., & Li, W. (2012). A color-coding amacrine cell may provide a blue-off signal in a mammalian retina. *Nature Neuroscience*, 15(7), 954–956.

Find this resource:

Chen, Q., Pei, Z., Koren, D., & Wei, W. (2016). Stimulus-dependent recruitment of lateral inhibition underlies retinal direction selectivity. *eLife*. 5, e21053.

Find this resource:

Chichilnisky, E. J. (2001). A simple white noise analysis of neuronal light. *Network*, 12, 199–213.

Find this resource:

Chichilnisky, E. J., & Baylor, D. (1999). Receptive-field microstructure of blue-yellow ganglion cells in primate retina. *Nature Neuroscience*, *2*(10), 889–893.

Find this resource:

Cook, J. E., & Becker, D.L. (1995). Gap junctions in the vertebrate retina. *Microscopy Research & Technique*, *31*(5), 408–419.

Find this resource:

Coombs, J. et al. (2006). Morphological properties of mouse retinal ganglion cells. *Neuroscience*, *140*(1), 123–136.

Find this resource:

Cronin, T.W., Johnsen, S., Marshall, N. J., & Warrant E. J. (2014). *Visual ecology*. 1st ed. Princeton, NJ: Princeton University Press.

Find this resource:

Crook, J. D., Davenport, C. M., Peterson, B. B., Packer, O. S., Detwiler, P. B., & Dacey, D. M. (2009). Parallel ON and OFF cone bipolar inputs establish spatially coextensive receptive field structure of blue-yellow ganglion cells in primate retina. *The Journal of Neuroscience*, *29*(26), 8372–8387.

Find this resource:

Crook, J. D., Manookin, M. B., Packer, O. S., & Dacey, D. M. (2011). Horizontal cell feedback without cone type-selective inhibition mediates ‘red-green’ color opponency in midget ganglion cells of the primate retina. *The Journal of Neuroscience*, *31*(5), 1762–1772.

Find this resource:

Dacey, D., Packer, O. S., Diller, L., Brainard, D., Peterson, B., Lee, B. (2000). Center surround receptive field structure of cone bipolar cells in primate retina. *Vision Research*, *40*(14), 1801–1811.

Find this resource:

Dacey, D. M. (2000). Parallel pathways for spectral coding in primate retina. *Annual Review of Neuroscience*, *23*, 743–775.

Find this resource:

Dacey, D. M., & Lee, B. B. (1994). The ‘blue-on’ opponent pathway in primate retina originates from a distinct bistratified ganglion cell type. *Nature*, *367*(6465), 731–735.

Find this resource:

Dacey, D. M., & Packer, O. S. (2003). Colour coding in the primate retina: Diverse cell types and cone-specific circuitry. *Current Opinion in Neurobiology*, *13*(4), 421–427.

Find this resource:

Dacheux, R. F., & Raviola, E. (1986). The rod pathway in the rabbit retina: A depolarizing bipolar and amacrine cell. *The Journal of Neuroscience*, *6*(2), 331–345.

Find this resource:

Demb, J. B. (2002). Multiple mechanisms for contrast adaptation in the retina. *Neuron*, *36*(5), 781–783.

Find this resource:

Demb, J. B. (2008). Functional circuitry of visual adaptation in the retina. *Journal of Physiology*, 586(Pt. 18), 4377–4384.

Find this resource:

Denton, E. J., & Wyllie, J. H. (1955). Study of the photosensitive pigments in the pink and green rods of the frog. *Journal of Physiology*, 127(1), 81–89.

Find this resource:

DeVries, S. H., & Schwartz, E. A. (1999). Kainate receptors mediate synaptic transmission between cones and ‘off’ bipolar cells in a mammalian retina. *Nature*, 397(6715), 157–160.

Find this resource:

DeVries, S. H. (2000). Bipolar cells use kainate and AMPA receptors to filter visual information into separate channels. *Neuron*, 28(3), 847–856.

Find this resource:

DeVries, S. H. (2001). Exocytosed protons feedback to suppress the Ca²⁺ current in mammalian cone photoreceptors. *Neuron*, 32, 1107–1117.

Find this resource:

Dhande, O. S., & Huberman, A. D. (2014). Retinal ganglion cell maps in the brain: Implications for visual processing. *Current Opinion in Neurobiology*, 24(1), 133–142.

Find this resource:

Ding, H., Smith, R. G., Poleg-Polsky, A., Diamond, J. S., & Briggman, K. L. (2016). Species-specific wiring for direction selectivity in the mammalian retina. *Nature*, 535(7610), 105–110.

Find this resource:

Donner, K. (1992). Noise and the absolute thresholds of cone and rod vision. *Vision Research*, 32(5), 853–866.

Find this resource:

Dowling, J. E. (1991). Retinal neuromodulation: The role of dopamine. *Visual Neuroscience*, 7, 87–97.

Find this resource:

Dryja, T. P., McGee, T. L., Berson, E. L., Fishman, G., Sandberg, M., Alexander, K. R., ... Rajagopalan, A. S. (2005). Night blindness and abnormal cone electroretinogram ON responses in patients with mutations in the GRM6 gene encoding mGluR6. *Proceedings of the National Academy of Sciences of the United States of America*, 102(13), 4884–4889.

Find this resource:

Dunn, F., Lankheet, M. J., & Rieke, F. (2007). Light adaptation in cone vision involves switching between receptor and post-receptor sites. *Nature*, 449(7162), 603–606.

Find this resource:

Eggers, E. D., & Lukasiewicz, P. D. (2011). Multiple pathways of inhibition shape bipolar cell responses in the retina. *Visual Neuroscience*, 28(1), 95–108.

Find this resource:

Eggers, E. D., McCall, M. A., & Lukasiewicz, P. D. (2007). Presynaptic inhibition differentially shapes transmission in distinct circuits in the mouse retina. *The Journal of Physiology*, 582(Pt. 2), 569–582.

Find this resource:

Emond, M. P., McNeil, R., Cabana, T., Guerra, C. G., & Lachapelle, P. (2006). Comparing the retinal structures and functions in two species of gulls (*Larus delawarensis* and *Larus modestus*) with significant nocturnal behaviours. *Vision Research*, 46(18), 2914–2925.

Find this resource:

Esposti, F., Johnston, J., Rosa, J. M., Leung, K. M., & Lagnado, L. (2013). Olfactory stimulation selectively modulates the OFF pathway in the retina of zebrafish. *Neuron*, 79(1), 97–110.

Find this resource:

Euler, T., Detwiler, P. B., & Denk, W. (2002). Directionally selective calcium signals in dendrites of starburst amacrine cells. *Nature*, 418(6900), 845–852.

Find this resource:

Euler, T., Haverkamp, S., Schubert, T., & Baden, T. (2014). Retinal bipolar cells: Elementary building blocks of vision. *Nature Reviews: Neuroscience*, 15, 507–519.

Find this resource:

Fain, G. L., Matthews, H. R., Cornwall, M. C., & Koutalos, Y. (2001). Adaptation in vertebrate photoreceptors. *Physiological Reviews*, 81(1), 117–151.

Find this resource:

Fairhall, A. L., Burlingame, C. A., Narasimhan, R., Harris, R. A., Puchalla, J. L., & Berry, M. J. (2006). Selectivity for multiple stimulus features in retinal ganglion cells. *Journal of Neurophysiology*, 96(5), 2724–2738.

Find this resource:

Famiglietti, E. V., Jr. (1983). ‘Starburst’ amacrine cells and cholinergic neurons: mirror-symmetric on and off amacrine cells of rabbit retina. *Brain Research*, 261(1), 138–144.

Find this resource:

Farshi, P., Fyk-Kolodziej, B., Krolewski, D. M., Walker, P. D., Ichinose, T. (2015). Dopamine D1 receptor expression is bipolar cell type-specific in the mouse retina. *The Journal of Comparative Neurology*, 2079, 2059–2079.

Find this resource:

Field, G. D., Greschner, M., Gauthier, J. L., Rangel, C., Shlens, J., Sher, A., ... Chichilnisky, E. J. (2009). High-sensitivity rod photoreceptor input to the blue-yellow color opponent pathway in macaque retina. *Nature Neuroscience*, 12(9), 1159–1164.

Find this resource:

Field, G. D., Gauthier, J. L., Sher, A., Greschner, M., Machado, T. A., Jepson, L. H., ... Chichilniski, E. J. (2010). Functional connectivity in the retina at the resolution of photoreceptors. *Nature*, 467(7316), 673–677.

Find this resource:

Field, G. D. & Rieke, F. (2002). Mechanisms regulating variability of the single photon responses of mammalian

rod photoreceptors. *Neuron*, 35(4), 733–747.

Find this resource:

Fite, K.V., & Rosenfield-Wessels, S. (1975). A comparative study of deep avian foveas. *Brain Behavior Evolution*, 12, 97–115.

Find this resource:

Foster, D. H. (2011). Color constancy. *Vision Research*, 51(7), 674–700.

Find this resource:

Franke, K., Berens, P., Schubert, T., Bethge, M., Euler, T., & Baden, T. (2016). Inhibition decorrelates visual feature representations in the inner retina. *Nature*, 542, 439–444.

Find this resource:

Fraser, B., DuVal, M. G., Wang, H., & Allison, W. T. (2013). Regeneration of cone photoreceptors when cell ablation is primarily restricted to a particular cone subtype. *PLoS ONE*, 8(1), e55410.

Find this resource:

Freeman, J., Field, G. D., Li, P. H., Greschner, M., Gunning, D. E., Mathieson, K., ... Chichilniski, E. J. (2015). Mapping nonlinear receptive field structure in primate retina at single cone resolution. *eLife*, 4, 284–299.

Find this resource:

Fu, Y., & Yau, K. W. (2007). Phototransduction in mouse rods and cones. *Pflugers Archiv European Journal of Physiology*, 454(5), 805–819.

Find this resource:

Geisler, W. S. (2008). Visual perception and the statistical properties of natural scenes. *Annual Review of Psychology*, 59, 167–192.

Find this resource:

Ghosh, K. K., Bujan, S., Haverkamp, S., Feigenspan, A., Wässle, H. (2004). Types of bipolar cells in the mouse retina. *The Journal of Comparative Neurology*, 469(1), 70–82.

Find this resource:

Ghosh, K. K., & Grünert, U. (1999). Synaptic input to small bistratified (blue-ON) ganglion cells in the retina of a new world monkey, the marmoset *Callithrix jacchus*. *The Journal of Comparative Neurology*, 413(3), 417–428.

Find this resource:

Goldberg, A. F. X., Moritz, O. L., & Williams, D. S., 2016. Molecular basis for photoreceptor outer segment architecture. *Progress in Retinal and Eye Research*, 55, 52–81.

Find this resource:

Gollisch, T., & Meister, M. (2009). Review eye smarter than scientists believed: Neural Computations in circuits of the retina. *Neuron*, 65(2), 150–164.

Find this resource:

Greene, M. J., Kim, J. S., & Seung, H. S. (2016). Analogous convergence of sustained and transient inputs in parallel on and off pathways for retinal motion computation. *Cell Reports*, 14(8), 1892–1900.

Find this resource:

Griebel, U., & Peichl, L. (2003). Colour vision in aquatic mammals—facts and open questions. *Aquatic Mammals*, 291, 18–30.

Find this resource:

Grimes, W. N., Zhang, J., Graydon, C. W., Kachar, B., & Diamond J. S. (2010). Retinal parallel processors: More than 100 independent microcircuits operate within a single interneuron. *Neuron*, 65(6), 873–885.

Find this resource:

Hailman, J. P. (1976). Oildroplets in the eyes of adult anuran amphibians: A comparative survey. *Journal of Morphology*, 148(4), 453–468.

Find this resource:

Hartveit, E. (1997). Reciprocal synaptic transmission between rod bipolar cells and amacrine cells in the rat retina. *The Journal of Neurophysiology*, 23(6), 2923–2936.

Find this resource:

Haverkamp, S., Eldred W. D., Ottersen, O. P., Pow, D., & Ammermüller, J. (1997). Synaptic inputs to identified color-coded amacrine and ganglion cells in the turtle retina. *The Journal of Comparative Neurology*, 389(2), 235–248.

Find this resource:

Haverkamp, S., Grünert, U. & Wässle, H. (2000). The cone pedicle, a complex synapse in the retina. *Neuron*, 27(1), 85–95.

Find this resource:

Haverkamp, S. & Wässle, H., (2004). Characterization of an amacrine cell type of the mammalian retina immunoreactive for vesicular glutamate transporter 3. *The Journal of Comparative Neurology*, 468(2), 251–263.

Find this resource:

Haverkamp, S., Wässle, H., Duebel, J., Kuner, T., Augustine, G. J., Feng, G., & Euler, T. (2005). The primordial, blue-cone color system of the mouse retina. *The Journal of Neuroscience*, 25(22), 5438–5445.

Find this resource:

He, S., Weiler, R., & Vaney, D. I., (2000). Endogenous dopaminergic regulation of horizontal cell coupling in the mammalian retina. *The Journal of Comparative Neurology*, 418(1), 33–40.

Find this resource:

Heitman, A., Brackbill, N., Greschner, N., Sher, A., Litke, E. J., Chichilniski, E. J. (2016). **Testing pseudo-linear models of responses to natural scenes in primate retina.** *bioRxiv*.

Find this resource:

Helmstaedter, M., Briggman, K. L., Turaga, S. C., Jain, V., Seung, H. S., & Denk, W. (2013). Connectomic reconstruction of the inner plexiform layer in the mouse retina. *Nature*, 500(7461), 168–174.

Find this resource:

Hensley, S. H., Yang, X. L., & Wu, S. M. (1993). Relative contribution of rod and cone inputs to bipolar cells and

ganglion cells in the tiger salamander retina. *The Journal of Neurophysiol*, 69(6), 2086–2098.

Find this resource:

Hoefflinger, B. (2007). The eye and high-dynamic-range vision. In *High-dynamic-range (HDR) vision* (pp. 1–12). Berlin and Heidelberg, Germany: Springer.

Find this resource:

Hurvich, L. M., & Jameson, D. (1957). An opponent-process theory of color vision. *Psychological Review*, 64(6), 384–404.

Find this resource:

Jackman, S. L., Babai, N., Chambers, J. J., Thoreson, W. B., Kramer, R. H. (2011). A positive feedback synapse from retinal horizontal cells to cone photoreceptors. *PLoS Biology*, 9(5), e1001057.

Find this resource:

Jacobs, G., Williams, G. A., Cahill, H., Nathans, J. (2007). Emergence of novel color vision in mice engineered to express a human cone photopigment. *Science*, 315(5819):1723-5.

Find this resource:

Jacobs, G. H. (1993). The distribution and nature of colour vision among the mammals. *Biological Reviews of the Cambridge Physiological Society*, 68(3), 413–471.

Find this resource:

Jacobs, G. H., & Rowe, M. P. (2004). Evolution of vertebrate colour vision. *Clinical and Experimental Optometry*, 87(4–5), 206–216.

Find this resource:

Jacoby, R., Stafford, D., Kouyama, N., & Marshak, D. (1996). Synaptic inputs to on parasol ganglion cells in the primate retina. *The Journal of Neuroscience*, 16(24), 8041–8056.

Find this resource:

Jian Wei Xu, J. W., & Slaughter, M. M. (2005). Large-conductance calcium-activated potassium channels facilitate transmitter release in salamander rod synapse. *The Journal of Neuroscience*, 25(33), 7660–7668.

Find this resource:

Jin, N.G., Ge, N., Chuang, A. Z., Masson, P. J., & Ribelayga, C. P. (2015). Rod electrical coupling is controlled by a circadian clock and dopamine in mouse retina. *Journal of Physiology*, 593(7), 1597–1631.

Find this resource:

Joesch, M., & Meister, M. (2016). A neuronal circuit for colour vision based on rod–cone opponency. *Nature*, 532(7598).

Find this resource:

Jusuf, P. R., Martin, P. R., & Grünert, U. (2006). Random wiring in the midget pathway of primate retina. *The Journal of Neuroscience*, 26(15), 3908–3917.

Find this resource:

Kamermans, M., van Dijk, B.W., & Spekreijse, H. (1991). Color opponency in cone-driven horizontal cells in carp

retina. A specific pathway between cones and horizontal cells. *Journal of General Physiology*, 97(4), 819–843.

Find this resource:

Kastner, D. B., & Baccus, S. A., (2013). Spatial segregation of adaptation and predictive sensitization in retinal ganglion cells. *Neuron*, 79(3), 541–554.

Find this resource:

Kefalov, V., Fu, Y., Marsh-Armstrong, N., & Yau, K. W. (2003). Role of visual pigment properties in rod and cone phototransduction. *Nature*, 425(6957), 526–531.

Find this resource:

Kelber, A., Vorobyev, M., & Osorio, D. (2003). Animal colour vision—behavioural tests and physiological concepts. *Biological reviews of the Cambridge Philosophical Society*, 78(1), 81–118.

Find this resource:

Kemmler, R., Schultz, K., Dedek, K., Euler, T. & Schubert, T. (2014). Differential regulation of cone calcium signals by different horizontal cell feedback mechanisms in the mouse retina. *The Journal of Neuroscience*, 34(35), 11826–11843.

Find this resource:

Kim, K. J., & Rieke, F. (2003). Slow Na⁺ inactivation and variance adaptation in salamander retinal ganglion cells. *The Journal of Neuroscience*, 23(4), 1506–1516.

Find this resource:

Kim, I.-J., Zhang, Y., Yamagata, M., Meister, M., & Sanes, J. R. (2008). Molecular identification of a retinal cell type that responds to upward motion. *Nature*, 452(7186), 478–482.

Find this resource:

Kim, J. S., Greene, M. J., Zlateski, A., Lee, K., Richardson, M., Turaga, C. S., ... the EyeWriters. (2014). Space-time wiring specificity supports direction selectivity in the retina. *Nature*, 509(7500), 331–336.

Find this resource:

Kim, K. J., & Rieke, F. (2003). Slow Na⁺ inactivation and variance adaptation in salamander retinal ganglion cells. *The Journal of Neuroscience*, 23(4), 1506–1516.

Find this resource:

Koch, K.-W. (1992). Biochemical mechanism of light adaptation in vertebrate photoreceptors. *Trends in Biochemical Sciences*, 17(8), 307–311.

Find this resource:

Kolb, H., & Marshak, D. (2003). The midget pathways of the primate retina. *Documenta Ophthalmologica*, 106(1), 67–81.

Find this resource:

Kolb, H., Fernandez, E., Ammermüller, J., & Cuenca, N. (1995). Substance P—a neurotransmitter of amacrine and ganglion cells in the vertebrate retina. *Histology & Histopathology*, 10(4), 947–968.

Find this resource:

Kong, J. H., Fish, D. R., Rockhill, R. L., & Masland, R. H. (2005). Diversity of ganglion cells in the mouse retina: Unsupervised morphological classification and its limits. *The Journal of Comparative Neurology*, 489(3), 293–310.

Find this resource:

Korenyak, D. A., & Govardovskii, V. I. (2013). Photoreceptors and visual pigments in three species of newts. *Journal of Evolutionary Biochemistry and Physiology*, 49(4), 399–407.

Find this resource:

Kothmann, W. W., Massey, S. C., & O'Brien, J. (2009). Dopamine-stimulated dephosphorylation of connexin 36 mediates AII amacrine cell uncoupling. *Journal of Neuroscience*, 29(47), 14903–14911.

Find this resource:

Kouyama, N., & Marshak, D. (1992). Bipolar cells specific for blue cones in the macaque retina. *Journal of Neuroscience*, 12(4), 1233–1252.

Find this resource:

Kram, Y. A., Mantey, S., Corbo, J. C. (2010). Avian cone photoreceptors tile the retina as five independent, self-organizing mosaics. *PLoS ONE*, 5(2), e8992.

Find this resource:

Krauskopf, J., Williams, D. R., & Heeley, D. W. (1982). Cardinal directions of color space. *Vision Research*, 22(9), 1123–1131.

Find this resource:

Kuffler, S. W. (1953). Discharge patterns and functional organization of mammalian retina. *Physiology*, 16, 37–68.

Find this resource:

Land, M., & Nilson, D.-E. (2012). *Animal Eyes*. Oxford: Oxford University Press.

Find this resource:

Laughlin, S. B. (1989). The role of sensory adaptation in the retina. *Journal of Experimental Biology*, 146, 39–62.

Find this resource:

Lee, B. B. (1996). Receptive field structure in the primate retina. *Vision Research*, 36(5), 631–644.

Find this resource:

Lee, B. B., Martin, P. R., & Grünert, U. (2010). Retinal connectivity and primate vision. *Progress in Retinal and Eye Research*, 29(6), 622–639.

Find this resource:

Lee, H. (1886). On the tapetum lucidum. *Medico-Chirurgical Transactions*, 69, 239–245.

Find this resource:

Lee, S., Chen, L., Chen, M., Ye, M., Seal, R. P., Zhou, Z. J. (2014). An unconventional glutamatergic circuit in the retina formed by vGluT3 amacrine cells. *Neuron*, 84(4), 708–715.

Find this resource:

Lee, S., Zhang, Y., Chen, M., Zhou, Z. J. (2016). Segregated glycine-glutamate co-transmission from vGluT3

amacrine cells to contrast-suppressed and contrast-enhanced retinal circuits. *Neuron*, 90(1), 27–34.

Find this resource:

Leskov, I. B., Klenchin, V. A., Handy, J. W., Whitlock, G. G., Govardovskii, V. I., Bownds, M. D., ... Arshavsky, V. Y. (2000). The gain of rod phototransduction: Reconciliation of biochemical and electrophysiological measurements. *Neuron*, 27(3), 525–537.

Find this resource:

Lettvin, J., Maturana, H., McCulloch, W., Pitts, W. (1959). What the frog's eye tells the frog's brain. *Proceedings of the IRE*, 47(11), 1940–1951.

Find this resource:

Li, W., & DeVries, S. H. (2004). Separate blue and green cone networks in the mammalian retina. *Nature Neuroscience*, 7(7), 751–756.

Find this resource:

Li, W., & DeVries, S. H. (2006). Bipolar cell pathways for color and luminance vision in a dichromatic mammalian retina. *Nature Neuroscience*, 9(5), 669–675.

Find this resource:

Li, Y. N., Tsujimura, T., Kawamura, S., & Dowling, J. E. (2012). Bipolar cell-photoreceptor connectivity in the zebrafish (*Danio rerio*) retina. *Journal of Comparative Neurology*, 520(16), 3786–3802.

Find this resource:

Liu, J. K., & Gollisch, T. (2015). Spike-triggered covariance analysis reveals phenomenological diversity of contrast adaptation in the retina. *PLOS Computational Biology*, 11(7), e1004425.

Find this resource:

Liu, X., Hirano, A. A., Sun, X., Brecha, N. C., & Barnes, S. (2013). Calcium channels in rat horizontal cells regulate feedback inhibition of photoreceptors through an unconventional GABA- and pH-sensitive mechanism. *The Journal of Physiology*, 591(13), 3309–3324.

Find this resource:

Liu, X., Grove, J. C. R., Hirano, A. A., Brecha, N. C., & Barnes, S. (2016). Dopamine D1 receptor modulation of calcium channel currents in horizontal cells of mouse retina. *The Journal of Neurophysiology*, 116(2), 686–697.

Find this resource:

Luo, D.-G., Xue, T., & Yau, K.-W. (2008). How vision begins: An odyssey. *Proceedings of the National Academy of Sciences of the United States of America*, 105(29), 9855–9862.

Find this resource:

MacNeil, M. A., & Masland, R. H. (1998). Extreme diversity among amacrine cells: Implications for function. *Neuron*, 20, 971–982.

Find this resource:

Makous, W. (2007). Emergence of novel color vision in mice engineered to express a human cone photopigment. *Science*, 318(5848), 196b.

Find this resource:

Mangel, S. C., & Dowling, J. E. (1985). Responsiveness and receptive field size of carp horizontal cells are reduced by prolonged darkness and dopamine. *Science*, *229*(4718), 107–1109.

Find this resource:

Manookin, M. B., & Demb, J. B. (2006). Presynaptic mechanism for slow contrast adaptation in mammalian retinal ganglion cells. *Neuron*, *50*(3), 453–464.

Find this resource:

Matthews, G., & Watanabe, S. (1987). Properties of ion channels closed by light and opened by guanosine 3'-5'-cyclic monophosphate in toad retinal rods. *The Journal of Physiology*, *389*, 691–715.

Find this resource:

Mariani, A. P. (1984). Bipolar cells in monkey retina selective for the cones likely to be blue-sensitive. *Nature*, *308*(5955), 184–186.

Find this resource:

Martin, P. R., Lee, B. B., White, A. J. R., Solomon, S. G., & Rüttiger, L. (2001). Chromatic sensitivity of ganglion cells in the peripheral primate retina. *Nature*, *410*(6831), 933–936.

Find this resource:

Masland, R. H. (1988). Amacrine cells. *Trends in Neurosciences*, *11*(9), 405–410.

Find this resource:

Masland, R. H. (2001). The fundamental plan of the retina. *Nature Neuroscience*, *4*(9), 877–886.

Find this resource:

Masland, R. H. (2005). The many roles of starburst amacrine cells. *Trends in Neurosciences*, *28*(8), 395–396.

Find this resource:

Masland, R. H. (2012). The tasks of amacrine cells. *Visual Neuroscience*, *29*(1), 3–9.

Find this resource:

Masland, R. H., Mills, J. W., & Cassidy, C. (1984). The functions of acetylcholine in the rabbit retina. *Proceedings of the Royal Society of London—Series B: Biological Sciences*, *223*(1230), 121–139.

Find this resource:

Masland, R. H., Mills, J. W., & Hayden, S. A. (1984). Acetylcholine-synthesizing amacrine cells: Identification and selective staining by using radioautography and fluorescent markers. *Proceedings of the Royal Society London B: Biological Sciences*, *223*(1230), 79–100.

Find this resource:

McFarland, J. M., Cui, Y., & Butts, D. A. (2013). Inferring nonlinear neuronal computation based on physiologically plausible inputs. *PLoS Computational Biology*, *9*(7), e1003143.

Find this resource:

Meister, M., & Berry, M. J. (1999). The neural code of the retina. *Neuron*, *22*(3), 435–450.

Find this resource:

Mills, J. W., & Massey, S. C. (1995). Differential properties of two ganglionic pathways made by AII amacrine

cells. *Nature*, 377(6551), 734–737.

Find this resource:

Mills, S. L., Tian, L. M., Hoshi, H., Whitaker, C. M., & Massey, S. C. (2014). Three distinct blue-green color pathways in a mammalian retina. *Journal of Neuroscience*, 34(5), 1760–1768.

Find this resource:

Mirauccourt, L. S., Tsui, J., Gobert, D., Desjardins, J. F., Schohl, A., Sild, M., ... Ruthazer, E. S., (2016). Endocannabinoid signaling enhances visual responses through modulation of intracellular chloride levels in retinal ganglion cells. *eLife*, 5, e15932.

Find this resource:

Mobbs, P., Everett, K., & Cook, A. (1992). Signal shaping by voltage-gated currents in retinal ganglion cells. *Brain Research*, 574(1–2), 217–223.

Find this resource:

Munch, T. A., da Silveira, R. A., Siebert, S., Viney, T. J., Awatramani, G. B. & Roska, B. (2009). Approach sensitivity in the retina processed by a multifunctional neural circuit. *Nature Neuroscience*, 12(10), 1308–1316.

Find this resource:

Naka, K. I., & Rushton, W. A. (1966). S-potentials from colour units in the retina of fish (Cyprinidae). *Journal of Physiology*, 185(3), 536–555.

Find this resource:

Nakajima, Y., Iwakabe, H., Akazawa, C., Nawa, H., Shigemoto, R., Mizuno, N., & Nakanishi, S. (1993). Molecular characterization of a novel retinal metabotropic glutamate receptor mGluR6 with a high agonist selectivity for L-2- amino-4-phosphonobutyrate. *Journal of Biological Chemistry*, 268(16), 11868–11873.

Find this resource:

Nathans, J. (1999). The evolution and physiology of human review color vision: Insights from molecular genetic studies of visual pigments. *Neuron*, 24, 299–312.

Find this resource:

Neitz, J., & Neitz, M., (2011). The genetics of normal and defective color vision. *Vision Research*, 51(7), 633–651.

Find this resource:

Nelson, R., & Kolb, H. (1983). Synaptic patterns and response properties of bipolar and ganglion cells in the cat retina. *Vision Research*, 23(10), 1183–1195.

Find this resource:

Nelson, R., & Kolb, H. (1985). A17: A broad-field amacrine cell in the rod system of the cat retina. *The Journal of Neurophysiology*, 54(3), 592–614.

Find this resource:

Nikolaev, A., Leung, K. M., Odermatt, B., & Lagnado, L. (2013). Synaptic mechanisms of adaptation and sensitization in the retina. *Nature Neuroscience*, 16(7), 934–941.

Find this resource:

Nikolaou, N., Lowe, A. S., Walker, A. S., Abbas, F., Hunter, P. R., Thompson, I. D., & Meyer, M. P. (2012). Parametric functional maps of visual inputs to the tectum. *Neuron*, *76*(2), 317–324.

Find this resource:

Normann, R. A., & Perlman, I. (1979). The effects of background illumination on the photoresponses of red and green cones. *The Journal of Physiology*, *286*, 491–507.

Find this resource:

Ollivier, F. J., Samuelson, D. A., Brooks, D. E., Lewis, P. A., Kallberg, M. E., & Komáromy, A. M. (2004). Comparative morphology of the tapetum lucidum (among selected species). *Veterinary Ophthalmology*, *7*(1), 11–22.

Find this resource:

Owens, G. L., Windsor, D. J., Mui, J., & Taylor, J. S., (2009). A fish eye out of water: Ten visual opsins in the four-eyed fish, *Anableps anableps*. *PLoS ONE*, *4*(6), e5970.

Find this resource:

Packer, O. S., Verweij, J., Li, P. H., Schnapf, J. L., & Dacey, D. M. (2010). Blue-yellow opponency in primate S cone photoreceptors. *The Journal of Neuroscience*, *30*(2), 568–572.

Find this resource:

Peichl, L. (1992). Topography of ganglion-cells in the dog and wolf retina. *The Journal of Comparative Neurology*, *324*(4), 603–620.

Find this resource:

Peichl, L. (2005). Diversity of mammalian photoreceptor properties: Adaptations to habitat and lifestyle? *The Anatomical Record. Part A: Discoveries in Molecular, Cellular, and Evolutionary Biology*, *287*(1), 1001–1012.

Find this resource:

Peichl, L., Künzle, H., & Vogel, P. (2000). Photoreceptor types and distributions in the retinæ of insectivores. *Visual Neuroscience*, *17*(6), 937–948.

Find this resource:

Peichl, L., Sandmann, D., & Boycott, B. B. (1998). Comparative anatomy and function of mammalian horizontal cells. In *Development and organization of the retina*. NATO ASI Series vol. 299. Boston: Springer.

Find this resource:

Pillow, J. W., Shlens, J., Paninski, L., Sher, A., Litke, A. M., Chichilnisky, E. J., & Simoncelli, E. P. (2008). Spatio-temporal correlations and visual signalling in a complete neuronal population. *Nature*, *454*(7207), 995–999.

Find this resource:

Pugh, E. N., & Lamb, T. D. (2000). Phototransduction in vertebrate rods and cones: Molecular mechanisms of amplification, recovery and light adaptation. In *Handbook of biological physics* (Vol. 3, pp. 183–255). Elsevier.

Find this resource:

Puller, C., Ivanova, E., Euler, T., Haverkamp, S., Schubert, T. (2013). OFF bipolar cells express distinct types of dendritic glutamate receptors in the mouse retina. *Neuroscience*, *243*, 136–148.

Find this resource:

Puller, C., Ondreka, K., & Haverkamp, S. (2011). Bipolar cells of the ground squirrel retina. *The Journal of Comparative Neurology*, 519(4), 759–774.

Find this resource:

Qiao, S., Zhang, Z., Ribelayga, C. P., & Zhong, Y. (2016). Multiple cone pathways are involved in photic regulation of retinal dopamine. *Scientific Reports*, 6, 28916.

Find this resource:

Real, E., Asari, H., Gollisch, T., Meister, M. (2017). Neural circuit inference from function to structure. *Current Biology*, 27(2), 189–198.

Find this resource:

Redmond, T. M., Yu, S., Lee, E., Bok, D., Hamasaki, D., Chen, N., ... Pfeifer, K. (1998). Rpe65 is necessary for production of 11-cis-vitamin A in the retinal visual cycle. *Nature Genetics*, 20(4), 344–351.

Find this resource:

Reitner, A., Sharpe, L. T., & Zrenner, E. (1991). Is colour vision possible with only rods and blue-sensitive cones? *Nature*, 352(6338), 798–800.

Find this resource:

Robles, E., Laurell, E., & Baier, H. (2014). The retinal projectome reveals brain-area-specific visual representations generated by ganglion cell diversity. *Current Biology*, 24(18), 2085–2096.

Find this resource:

Röhlich, P., van Veen, T., & Szél, A. (1994). Two different visual pigments in one retinal cone cell. *Neuron*, 13(5), 1159–1166.

Find this resource:

Roorda, A., & Williams, D. R. (1999). The arrangement of the three cone classes in the living human eye. *Nature*, 397(6719), 520–522.

Find this resource:

Rosa, J. M., Ruehle, S., Ding, H., & Lagnado, L. (2016). Crossover inhibition generates sustained visual responses in the inner retina. *Neuron*, 90(2), 308–319.

Find this resource:

Roska, B. & Werblin, F., (2001). Vertical interactions across ten parallel, stacked representations in the mammalian retina. *Nature*, 410(6828), 583–587.

Find this resource:

Sabesan, R., Schmidt, B. P., Tuten, W. S., & Roorda, A. (2016). The elementary representation of spatial and color vision in the human retina. *Science Advances*, 2(9), e1600797–e1600797.

Find this resource:

Salbreux, G., Barthel, L. K., Raymond, P. A., & Lubensky D. K. (2012). Coupling mechanical deformations and planar cell polarity to create regular patterns in the Zebrafish retina. *PLoS Computational Biology*, 8(8), e1002618.

Find this resource:

Sanes, J. R., & Masland, R. H. (2014). The types of retinal ganglion cells: Current status and implications for neuronal classification. *Annual Review of Neuroscience*, *38*(1), 221–246.

Find this resource:

Santina, L. D., Kuo, S. P., Yoshimatsu, T., Okawa, H., Suzuki, S. C., Hoon, M., ... Wong, R. O. L. (2016). Glutamatergic monopolar interneurons: A novel pathway of excitation in the mouse retina. *Current Biology*, *26*(15), 2070–2077.

Find this resource:

Schwartz, G. W., Okawa, H., Dunn, F. A., Morgan, J. L., Kerschensteiner, D., Wong, R. O., & Rieke, F. (2012). The spatial structure of a nonlinear receptive field. *Nature Neuroscience*, *15*(11), 1572–1580.

Find this resource:

Schwartz, O., Pillow, J. W., Rust, N. C., Simoncelli, E. P. (2006). Spike-triggered neural characterization. *Journal of Vision*, *6*(4), 13.

Find this resource:

Shapley, R., & Victor, J. D. (1978). The effect of contrast on the transfer properties of cat retinal ganglion cells. *The Journal of Physiology*, *285*, 275–298.

Find this resource:

Sharpe, L. T. & Stockman, A., (1999). Rod pathways: The importance of seeing nothing. *Trends in Neurosciences*, *22*(11), 497–504.

Find this resource:

Shekhar, K., Lapan, S. W., Whitney, I. E., Tran, N. M., Macoski, E. Z., Kowalczyk, M., ... Sanes, J. R. (2016). Comprehensive classification of retinal bipolar neurons by single-cell transcriptomics. *Cell*, *166*(5), 1308–1323.

Find this resource:

Shen, Y., Kamermans, H. M., Peachey, N. S., Gregg, R. G., & Nawy, S. (2009). A transient receptor potential-like channel mediates synaptic transmission in rod bipolar cells. *The Journal of Neuroscience*, *29*(19), 6088–6093.

Find this resource:

Sher, A., & DeVries, S. H. (2012). A non-canonical pathway for mammalian blue-green color vision. *Nature Neuroscience*, *15*(7), 952–953.

Find this resource:

Shimokawa, T., Rogel, A., Pakdaman, K., & Sato, S. (1999). Stochastic resonance and spike-timing precision in an ensemble of leaky integrate and fire neuron models. *Physical Review E*, *59*(3), 3461–3470.

Find this resource:

Sivak, J. G. (1976). Optics of the eye of the ‘four-eyed fish’ (*Anableps anableps*). *Vision Research*, *16*(5), 531–534.

Find this resource:

Sivyer, B., Taylor, W. R., & Vaney, D. I. (2010). Uniformity detector retinal ganglion cells fire complex spikes and receive only light-evoked inhibition. *Proceedings of the National Academy of Sciences of the United States of America*, *107*(12), 5628–5633.

Find this resource:

Smallwood, P. M., Olveczky, B. P., Williams, G. L., Jacobs, G. H., Reese, B. E., Meister, M., & Nathans, J. (2003). Genetically engineered mice with an additional class of cone photoreceptors: Implications for the evolution of color vision. *Proceedings of the National Academy of Sciences*, *100*(20), 11706–11711.

Find this resource:

Soo, F. S., Detwiler, P. B., & Rieke, F. (2008). Light adaptation in salamander l-cone photoreceptors. *The Journal of Neuroscience*, *28*(6), 1331–1342.

Find this resource:

Sterling, P., & Laughlin, S. B. (2016). Principles of neural design. MIT press.

Find this resource:

Sterling, P., & Matthews, G. (2005). Structure and function of ribbon synapses. *Trends in Neurosciences*, *28*(1), 20–29.

Find this resource:

Sümbül, U., Song, S., McCulloch, K., Becker, M, Lin, B., Sanes, J. R., ... Seung, H. S. (2014). A genetic and computational approach to structurally classify neuronal types. *Nature Communications*, *5*, 3512.

Find this resource:

Sun, W., Li, N., & He, S. (2002). Large-scale morphological survey of mouse retinal ganglion cells. *Journal of Comparative Neurology*, *451*(2), 115–126.

Find this resource:

Swamynathan, S. K., Crawford, M. A., Robison, W. G., Kanungo, J., & Piatigorsky, J. (2003). Adaptive differences in the structure and macromolecular compositions of the air and water corneas of the ‘four-eyed’ fish (*Anableps anableps*). *The FASEB Journal*, *17*(14), 1996–2005.

Find this resource:

Szél, A., & Roehlich, P. (1992). Two cone types of rat retina detected by anti-visual pigment antibodies. *Experimental Eye Research*, *55*, 47–52.

Find this resource:

Szél, A., Röhlich, P., Caffé, A. R., Juliusson, B., Aguirre, G., & Van Veen, T. (1992). Unique topographic separation of two spectral classes of cones in the mouse retina. *Journal of Comparative Neurology*, *325*(3), 327–342.

Find this resource:

Szmajda, B. A. & DeVries, S. H. (2011). Glutamate spillover between mammalian cone photoreceptors. *Journal of Neuroscience*, *31*(38), 13431–13441.

Find this resource:

Thoen, H. H., How, M. J., Chiou, T. H., & Marshall, J. (2014). A different form of color vision in mantis shrimp. *Science*, *343*, 411–413.

Find this resource:

Thoreson, W. B., & Mangel, S. C. (2012). Lateral interactions in the outer retina. *Progress in Retinal and Eye Research*, 31(5), 407–441.

Find this resource:

Tien, N.-W., Kim, T., & Kerschensteiner, D. (2016). Target-specific glycinergic transmission from VGluT3-expressing amacrine cells shapes suppressive contrast responses in the retina. *Cell Reports*, 15(7), 1369–1375.

Find this resource:

Tien, N.-W., Pearson, J. T., Heller, C. R., Demas, J., & Kerschensteiner, D. (2015). Genetically identified suppressed-by-contrast retinal ganglion cells reliably signal self-generated visual stimuli. *The Journal of Neuroscience*, 35(30), 10815–10820.

Find this resource:

Tyrrell, L. P. Moore, B. A., Loftis, C., & Fernandez-Juricic, E. (2013). Looking above the prairie: localized and upward acute vision in a native grassland bird. *Scientific Reports*, 3, 128–145.

Find this resource:

Urschel, S., Hoher, T., Schubert, T., Alev, C., Sohl, G., Worsdorfer, P., ... Willecke, K. (2006). Protein kinase A-mediated phosphorylation of connexin36 in mouse retina results in decreased gap junctional communication between AII amacrine cells. *Journal of Biological Chemistry*, 281(44), 33163–33171.

Find this resource:

Vaney, D. I. (1990). The mosaic of amacrine cells in the mammalian retina. *Progress in Retinal Research*, 9, 49–100.

Find this resource:

Vaney, D. I., Nelson, J. C., & Pow, D. V. (1998). Neurotransmitter coupling through gap junctions in the retina. *The Journal of Neuroscience*, 18(24), 10594–10602.

Find this resource:

Vaney, D. I., Sivyer, B., & Taylor, W. R. (2012). Direction selectivity in the retina: Symmetry and asymmetry in structure and function. *Nature Reviews: Neuroscience*, 13(3), 194–208.

Find this resource:

Ventura, D. F., Zana, Y., Souza, J. M., DeVoe, R. D. (2001). Ultraviolet colour opponency in the turtle retina. *Journal of Experimental Biology*, 204(14), 2527–2534.

Find this resource:

Verweij, J., Hornstein, E. P. & Schnapf, J. L. (2003). Surround antagonism in macaque cone photoreceptors. *Journal of Neuroscience*, 23(32), 10249–10257.

Find this resource:

Vickers, E., Kim, M. H., Vigh, J., von Gersdorff, H. (2012). Paired-pulse Plasticity in the strength and latency of light-evoked lateral inhibition to retinal bipolar cell terminals. *The Journal of Neuroscience*, 32(34), 11688–11699.

Find this resource:

Von Schantz, M., Argamaso-Hernan, S. M., Szel, A., & Foster, R. G. (1997). Photopigments and photoentrainment in the Syrian golden hamster. *Brain Research*, 770(1–2), 131–138.

Find this resource:

Völgyi, B., Chheda, S., & Bloomfield, S.A. (2009). Tracer coupling patterns of the ganglion cell subtypes in the mouse retina. *Journal of Comparative Neurology*, 512(5), 664–687.

Find this resource:

Vroman, R., Klaassen, L. J., Howlett, M. H. C., Cenedese, V., Klooster, J., Sjoerdsma, T., & Kamermans, M. (2014). Extracellular ATP hydrolysis inhibits synaptic transmission by increasing pH buffering in the synaptic cleft. *PLoS Biology*, 12(5), e1001864.

Find this resource:

Vroman, R., & Kamermans, M. (2015). Feedback-induced glutamate spillover enhances negative feedback from horizontal cells to cones. *Journal of Physiology*, 593(13), 2927–2940.

Find this resource:

Wark, B., Fairhall, A., & Rieke, F. (2009). Timescales of inference in visual adaptation. *Neuron*, 61(5), 750–761.

Find this resource:

Wässle, H. (2004). Parallel processing in the mammalian retina. *Nature Reviews: Neuroscience*, 5(10), 747–757.

Find this resource:

Wässle, H., Puller, C., Müller, F., & Haverkamp, S. (2009). Cone contacts, mosaics, and territories of bipolar cells in the mouse retina. *Journal of Neuroscience*, 29(1), 106–117.

Find this resource:

Webster, M. (2011). Adaptation and visual coding. *Journal of Vision*, 11(5), 1–23.

Find this resource:

Weick, M., & Demb, J. B. (2011). Delayed-rectifier K channels contribute to contrast adaptation in mammalian retinal ganglion cells. *Neuron*, 71(1), 166–179.

Find this resource:

Weiler, R., Schultz, K., Pottek, M., Tieding, S., & Janssen-Bienhold, U. 1998. Retinoic acid has light-adaptive effects on horizontal cells in the retina. *Proceeding of the National Academy of Sciences U S A*, 95(12), 7139–7144.

Find this resource:

Werblin, F. S., & Dowling, J. E. (1969). Organization of the retina of the mudpuppy, *Necturus maculosus*. II. Intracellular recording. *The Journal of Neurophysiology*, 32(3), 339–355.

Find this resource:

Williams, R. W., Strom, R. C. & Goldowitz, D. (1998). Natural variation in neuron number in mice is linked to a major quantitative trait locus on Chr 11. *Journal of Neuroscience*, 18(1), 138–146.

Find this resource:

Yau, K.W., Lamb, T. D., Matthews, G., & Baylor, D.A. (1979). Current fluctuations across single rod outer segments. *Vision Research*, 19(4), 387–390.

Find this resource:

Yau, K.-W., & Hardie, R. C. (2009). Phototransduction Motifs and Variations. *Cell*, 139(2), 246–264.

Find this resource:

Yazulla, S. (2008). Endocannabinoids in the retina: From marijuana to neuroprotection. *Progress in Retinal and Eye Research*, 27(5), 501–526.

Find this resource:

Yin, L., Smith, R. G., Sterling, P., & Brainard, D. H. (2009). Physiology and morphology of color-opponent ganglion cells in a retina expressing a dual gradient of S and M opsins. *The Journal of Neuroscience*, 29(9), 2706–2724.

Find this resource:

Zhang, Y., Kim, I. J., Sanes, J. R., & Meister, M. (2012). The most numerous ganglion cell type of the mouse retina is a selective feature detector. *Proceedings of the National Academy of Sciences of the United States of America*, 109(36), E2391–E2398.

Find this resource:

Zrenner, E., & Gouras, P. (1981). Characteristics of the blue sensitive cone mechanism in primate retinal ganglion cells. *Vision Research*, 21(11), 1605–1609.

Find this resource:

Tom Baden

School of Life Sciences, University of Sussex and Institute of Ophthalmic Research, University of Tübingen

Timm Schubert

Werner Reichardt Centre for Integrative Neuroscience, University of Tübingen

Philipp Berens

Institute for Ophthalmic Research, University of Tübingen

Thomas Euler

Werner Reichardt Centre for Integrative Neuroscience, University of Tübingen

PRINTED FROM the OXFORD RESEARCH ENCYCLOPEDIA, NEUROSCIENCE (neuroscience.oxfordre.com). (c) Oxford University Press USA, 2016. A see applicable Privacy Policy and Legal Notice.

Subscriber: University of Sussex; date: 03 April 2018



